

Combustion completeness and sample location determine wildfire ash leachate chemistry

Micheline Campbell¹, Pauline C. Treble^{2,1}, Liza K. McDonough², Sebastian Naeher³, Andy Baker^{1,2}, Pauline F. Grierson⁴, Henri Wong², and Martin S. Andersen⁵.

¹School of Biological, Earth, and Environmental Sciences, UNSW Sydney, Sydney, Australia.

²ANSTO, Lucas Heights, Australia

³GNS Science, Lower Hutt, New Zealand

⁴School of Biological Sciences, The University of Western Australia, Perth, Australia

⁵Water Research Laboratory, School of Civil and Environmental Engineering, UNSW Sydney, Sydney, Australia

Corresponding author: Micheline Campbell (micheline.campbell@unsw.edu.au)

Key points

- Stalagmites record past fire activity through changes in inorganic and organic chemistry, sourced from ashes.
- Wildfire ash leachate chemistry will aid interpretation of proxy fire data.
- Results show inorganic chemistry varies with burn severity and sample location, pyrogenic biomarker signal is less clear.

Abstract

Understanding past fire regimes and how they vary with climate, human activity, and vegetation patterns is fundamental to the mitigation and management of changing fire regimes as anthropogenic climate change progresses. Ash-derived trace elements and pyrogenic biomarkers from speleothems have recently been shown to record past fire activity in speleothems from both Australia and North America. This calls for an empirical study of ash geochemistry to aid the interpretation of speleothem palaeofire proxy records. Here we present analyses of leached ashes collected following fires in southwest and southeast Australia. We include a suite of inorganic elemental data from the water-soluble fraction of ash, as well as a selection of organic analytes (pyrogenic lipid biomarkers). We also present elemental data from leachates of soils collected from sites in southwest Australia. We demonstrate that the water-soluble fraction of ash differs from the water-soluble fraction of soils, with trace and minor element concentrations in ash leachates varying with combustion completeness (burn severity) and sample location. Changes in some lipid biomarker concentrations extracted from ashes may reflect burn severity. Our results contribute to building a process-based understanding of how speleothem geochemistry may record fire frequency and severity, and suggest that more research is needed to understand the transport pathways for the inclusion of pyrogenic biomarkers in speleothems. Our results also demonstrate that potential contaminant loads from ashes are much higher than from soils, with implications for the management of karst catchments, which are a critical water resource.

Plain Language Summary

Understanding past fire activity is necessary to develop effective land management strategies to both manage activity. Recently, stalagmites (naturally forming cave decorations) have been shown to record past fire information through chemical changes. The chemical

changes are due to post-fire leaching of wildfire ash. By investigating wildfire ash chemistry, we will be able to improve our interpretations of the stalagmite past fire signal. Our results show that ash chemistry from Australian fires varies with burn severity and sample location, and that the ash chemistry and soil chemistry differ. Results suggest stalagmites may record burn severity as well as fire frequency. We also suggest that the potential impact of high concentrations of potential contaminants in wildfire ash on karst aquifers should be further investigated.

1 Introduction

Wildfires occur on all ice-free continents, affecting about 40% of the terrestrial biome (Chapin et al., 2011). Each year, an estimated ~300-460 million ha burn globally (Giglio et al., 2006; Lizundia-Loiola et al., 2020; Wei et al., 2021). Globally, there has been an observed increase in fire weather which has contributed to an increase in burned area in some regions (noting that fire occurrence is modulated by more than just dangerous fire weather) (Jones et al., 2022). Observational records are too short to fully understand fire regimes, so proxy palaeofire data are sourced from natural archives such as sediment cores, ice cores, and tree scars. These proxy archives have allowed past fire activity to be reconstructed at local (e.g. Rehn et al., 2021), continental (e.g. Zennaro et al., 2015), and global scales (e.g. Marlon et al., 2008).

Recent studies have shown that speleothems (cave formations such as stalagmites) can record past fire activity via changes in both inorganic and organic chemistry. The inorganic chemistry of karst dripwaters was shown to vary with cave depth, hydrogeology, and fire severity (e.g. Treble et al. 2016; Nagra et al. 2016; Bian et al. 2019; Coleborn et al. 2018, 2019), with the strongest response in the most proxies observed in a shallow cave after a severe fire (Bian et al. 2019). McDonough et al. (2022) demonstrated that an annually-laminated stalagmite collected from a cave in Yanchep National Park, southwest Australia, recorded all known fires to have burned over the cave through a suite of trace elements (notably transition metals), colloidal organic matter content, growth rate, calcite $\delta^{18}\text{O}$, and stalagmite fabrics. The annually laminated speleothem allowed for a coupled reconstruction of past fire and climate, at very high resolution (annual resolution with a maximum age uncertainty of ± 13 years over the 246-year long record) (McDonough et al., 2022). The potential to reconstruct past fires at such high resolution and over long time periods distinguishes speleothems from traditional palaeofire archives, which may be long, or high-resolution, but rarely both (see Campbell et al. (2023)). Other research efforts have focused on pyrogenic biomarkers, such as levoglucosan and polycyclic aromatic hydrocarbons (PAHs) (Argiriadis et al., 2023, 2019; Homann et al., 2023, 2022), where elevated concentrations of these pyrogenic biomarkers in speleothem calcite have been attributed to past fire events. Generally, it is supposed that both inorganic and organic fire proxies are sourced from ashes deposited over the cave, which are subsequently leached by rainfall, and transported via karst flowpaths and deposited with speleothem calcite. Refining the interpretation of speleothem palaeofire proxies calls for an empirical study of the geochemistry of ash to inform the interpretation of both organic and inorganic speleothem fire proxy records. While there are many studies of both laboratory and wildfire ash chemistry, particularly within the context of contamination risk, this has not been done either in karst environments or to understand ash chemistry within the context of speleothem palaeofire records. Understanding wildfire ash chemistry in the karst environment also has implications for water resources planning and contamination risk management.

Ash from combusted biomass is generally comprised of charred organic components and minerals. At lower temperatures (usually $<450\text{ }^{\circ}\text{C}$) ash is mostly comprised of organic

carbon, while at higher temperatures ($>450\text{ }^{\circ}\text{C}$), ash is comprised mostly of minerals as inorganic carbonates, and at very high temperatures ($>580\text{ }^{\circ}\text{C}$) most remaining minerals are present as oxides (Certini, 2005; Bodí et al., 2014). Ash colour is generally related to combustion completeness, with dark, organic-rich ashes formed at lower degrees of combustion, and lighter mineral-rich ashes formed due to greater combustion completeness (Bodí et al., 2014; Roy et al., 2010; Stronach and McNaughton, 1989). White ash is usually more alkaline than black ash due to the solubilisation of major elements in ash (Bodí et al., 2014; Pereira et al., 2012; Ulery et al., 1993), with ash pH generally ranging from 9.0 to 13.5 (Khanna et al., 1994; Misra et al., 1993; Yusiharni and Gilkes, 2012). Ash is an expected source of certain elements owing to their sequestration within plant biomass, both living and dead. Most biomass is comprised of C, with proportionally smaller amounts of H, O, N, P, and S. Elements such as K, Na, Ca, Mg, Mn and Cl are taken up from the soil as ions for functions including cellular structure and osmoregulation (Broadley et al., 2012; Kirkby, 2012). Fe, Mn, Cu and Zn are essential micronutrients but have low solubility, particularly in alkaline calcareous soils, thus their uptake from soil solution requires them to be in a chelated form. Calcium, Mg, K, Si, P, Na, S, Al, Fe, Mn, Zn, and associated carbonates (e.g., CaCO_3 , MgCO_3 , and K_2CO_3) are normally the dominant inorganic constituents of ash (Bodí et al., 2014; Gabet and Bookter, 2011; Pereira and Úbeda, 2010; Qian et al., 2009). However, their relative amounts and proportions of different elements vary considerably as different elements are volatilised to lesser or greater extent depending on the temperature of combustion (Bodí et al., 2014; Hogue and Inglett, 2012). Concentrations of elements in ash also reflects differences in sources, i.e., which tissues (leaf or wood) have been combusted, as well as variation among species (e.g. Yusiharni and Gilkes, 2012). In a global analysis, Sánchez-García et al. (2023) found that total extractable concentrations of the most abundant constituents (organic C, Ca, Al, Fe, N, Mg, Na, and P, in order of mean abundance) were variable, with large ranges. Mean concentrations ranged between 2.5 mg kg^{-1} (P) to 204 g kg^{-1} (organic C). Concentrations of the most abundant readily dissolvable constituents (organic C, Ca, Na, Mg, PO_4 , NH_4 , Al, F, Mn, and Fe) were also variable, and mean concentrations ranged between 1.3 mg kg^{-1} (Fe) to 1103 mg kg^{-1} (organic C). The ranges of the concentrations they reported were generally consistent with other (local) studies reported in the literature. Sánchez-García et al. (2023) reported that the variance in their ash concentrations was due to the ecosystem, burn severity, land use history (resulting in. legacy contamination) and leaching by rainfall prior to sample collection. Wildfires produce varying ash amounts. Reported ash loads in Australia range between 6 Mg ha^{-1} (Santín et al., 2015) to 115.6 Mg ha^{-1} (Santín et al., 2012), with ash load varying with burn severity and available fuel load (Santín et al., 2015, 2012). In experimental settings, hotter combustion temperatures have been shown to result in Ca/Mg ratios in ash leachates of <1 (Marion et al., 1991; Úbeda et al., 2009). However, in ashes from both experimental studies and wildfires with known burn temperature or severity (Balfour and Woods, 2013; Miotliński et al., 2023; Pereira et al., 2012; Sánchez-García et al., 2023; Santín et al., 2015; Úbeda et al., 2009), the response of both Ca and Mg to burn severity is variable, and none of the published concentrations support the hypothesis that this ratio indicates burn severity.

In speleothems, trace elements are derived from soil as well as soluble ash products. Fires affect soils in many ways, including alterations to soil organic matter (SOM), decreased cohesion, increased soil water repellence, and altered soil chemistry (Campos et al., 2015; Certini, 2005; DeBano, 2000; Pellegrini et al., 2022; Roshan and Biswas, 2023). Ash deposition has been shown to both directly and indirectly alter soil chemistry. Soil pH, exchangeable ions (Na^+ , K^+ , Ca^+ , and Mg^+), total N, and available PO_4 , are consistently higher post-fire, particularly in association with ash beds (Adams and Boyle, 1980; Certini, 2005; Humphreys and Lambert, 1965; Khanna et al., 1994; Serrasolsas and Khanna, 1995).

These effects can persist for months (e.g. Granged et al. (2011)) to years after fire (e.g. Muñoz-Rojas et al., 2016). Fire impact on soils is largely determined by fire intensity and duration, which is a function of the ecosystem and climate (Roshan and Biswas, 2023; Shakesby and Doerr, 2006). Surface soils also tend to be more affected than deeper soils (Bento-Gonçalves et al., 2012; Bradstock and Auld, 1995; Williams et al., 2004). Soil moisture further modulates both fire temperature at the soil surface and temperature penetration. In moist soils, temperatures tend to be lower until soil moisture is vapourised, however, moist soils tend to transport heat more quickly and therefore deeper (Campbell et al., 1994; Certini, 2005). Consequently, the impact of fires on soils, and the recovery of those soils to pre-fire conditions, is difficult to predict, and soil impacts and recovery are likely to vary in both time and space.

The legacies of fire impacts on ash and soil are also evident in organic compounds resulting from the combustion of plant material. Pyrogenic biomarkers such as levoglucosan and polycyclic aromatic hydrocarbons (PAHs) are used to investigate past fire activity in environmental archives such as ice and sediment cores, and speleothems (Argiriadis et al., 2019, 2023; Denis et al., 2012; Homann et al., 2022, 2023; Rubino et al., 2016; Vachula et al., 2019). Levoglucosan (1,6-anhydro- β -d-glucopyranose) is a water-soluble anhydrosugar which is formed through the thermal breakdown of cellulose and hemicellulose (Bhattarai et al., 2019; Elias et al., 2001; Li et al., 2021; Simoneit et al., 1999). Levoglucosan is source specific, and unlike other pyrogenic biomarkers, is not produced by the combustion of fossil fuels, making it a reliable tracer of biomass burning (Elias et al., 2001). While normally associated with particulate matter and smoke, levoglucosan has been shown to be present in black char (Kuo et al., 2008; Otto et al., 2006). Levoglucosan yield from black char has been shown to vary with temperature and plant species (Kuo et al., 2008). Levoglucosan is semi-volatile and can be transported with smoke in the atmosphere, where it has an atmospheric life of ~26 days (Bai et al., 2013). PAHs are organic molecules characterised by two or more aromatic rings which form by incomplete combustion of biomass and fossil fuels. In the modern era anthropogenic inputs (e.g. fossil fuels) are the dominant source, and in sediment cores the most recent deposits can be greatly enriched relative to pre-industrial levels (Perrette et al., 2008; Wakeham et al., 1980). The amount and type of PAHs formed by fire is controlled by the maximum temperature, duration, and oxygen level (Blumenstock et al., 2000; Johansson and van Bavel, 2003). At temperatures up to 400 °C, low molecular weight PAHs (<252 g/mol; 4-ring compounds) are more abundant in post-fire soils than high molecular weight PAHs (>252 g/mol; 5-ring compounds) (Kim et al., 2011; Rey-Salgueiro et al., 2018; Simon et al., 2016). Karp et al. (2020) describe a temperature optimum for PAH formation between 400 °C and 600 °C. Low PAH yield at low temperature is explained by incomplete condensation of ≤ 2 ring PAHs, while low yield at high temperature is explained by either complete combustion of the PAHs, or their incorporation into larger particles (>8 rings) (Karp et al., 2020). While PAHs adsorb onto organic matter, which limits degradation and bioavailability, levels in post-fire soils have been shown to decline to pre-fire concentrations over time as leaching and erosion mobilises PAHs (Kim et al., 2011; Simon et al., 2016; Yang et al., 2010). Degradation of PAHs has also been shown to occur in soil samples stored at ambient temperatures (Douglas et al., 2018; Rost et al., 2002). However, Douglas et al. (2018) showed that the PAHs chrysene and pyrene were resistant to degradation under ambient temperatures over the 30 day study. Some research has attributed high soil PAH levels to ash deposition, while others have suggested that the ash bed is not a source of PAHs for soils, and that PAHs are instead mobilised and transported to waterways rather than infiltrating (Kim et al., 2011; Simon et al., 2016). In speleothems, it is unclear whether the pyrogenic biomarker signal is transported via the leaching of deposited ashes over the cave, or via aerosol inputs (Homann et al., 2023), although Homann et al. (2022)

sampled cave dripwaters and demonstrated that in that cave levoglucosan was transported via the epikarst. Analyses of pyrogenic biomarkers in wildfire ash will contribute to building a process-based understanding of pyrogenic biomarkers as speleothem proxies.

Speleothems are excellent geochemical archives of past surface environmental change (e.g., Cheng et al., 2016; Domínguez-Villar et al., 2009). While speleothem proxies have recently been used to investigate past fire (see Argiriadis et al., 2023; Homann et al., 2023, 2022; McDonough et al., 2022), a process-based understanding of the formation of fire proxies (both organic and inorganic) and how they reflect fire activity is needed to 1) build confidence in speleothems as archives of past fire, and 2) determine whether and how speleothems can record past fire severity as well as frequency. Here we present analyses of inorganic proxies in the water-soluble fraction of ash and soil samples collected from southwest and southeast Australia, and organic pyrogenic biomarkers from the solvent-extracted fraction of ashes. We present a suite of elemental data, as well as electrical conductivity, pH, and alkalinity, for ash and soil leachates, as well as a limited number of pyrogenic biomarkers for a subset of ash samples. Results presented here will aid the interpretation of both organic and inorganic palaeofire proxy data in natural archives such as speleothems and sediment cores.

2 Site description and methods

2.1 Site descriptions

2.1.1 Southwest Australia

We collected ash and soil samples from two regions in southwest Australia: the Yanchep National Park in the Perth region and Leeuwin-Naturaliste National Park in the Capes region (Figure 1). Yanchep National Park is located ~47 km north of Perth, Western Australia. The underlying geology is the Tamala Limestone, a Pleistocene aeolianite (Playford et al., 1976). The climate is characteristically Mediterranean, with cool, wet winters and hot, dry summers, with most rainfall occurring during the winter (McDonough et al., 2022). Vegetation in the generally region follows a progression inland from dune vegetation dominated by sedges, rushes, and rhizomatous grasses, to coastal heath, limestone heath, and then *Banksia*-dominated woodland, with some wetland present (Fontaine, 2022). Eucalypt and *Melaleuca* woodlands are also widespread. Ash samples were collected at Yanchep in January 2020, following a severe wildfire in December 2019 from a region of the National Park where vegetation is comprised of a tuart (*Eucalyptus gomphocephalla*) overstorey with and understorey of *banksia* heath, interspersed by occasional wetland. The 2019 fire burned ~12300 ha, but with some variability, such that a range of severity classes are represented (Fontaine, 2022). An analysis of the differenced Normalised Burn Ratio (dNBR; see Text S1) shows that the most common severity class was ‘Moderate-high severity’, representing ~5200 ha (dNBR between 0.44 and 0.659; Key and Benson, 2006). See Text S1 for a dNBR map of this event. Soil samples were collected from two sites within Yanchep National Park in 2022, see Section 2.3 for the sampling protocol.

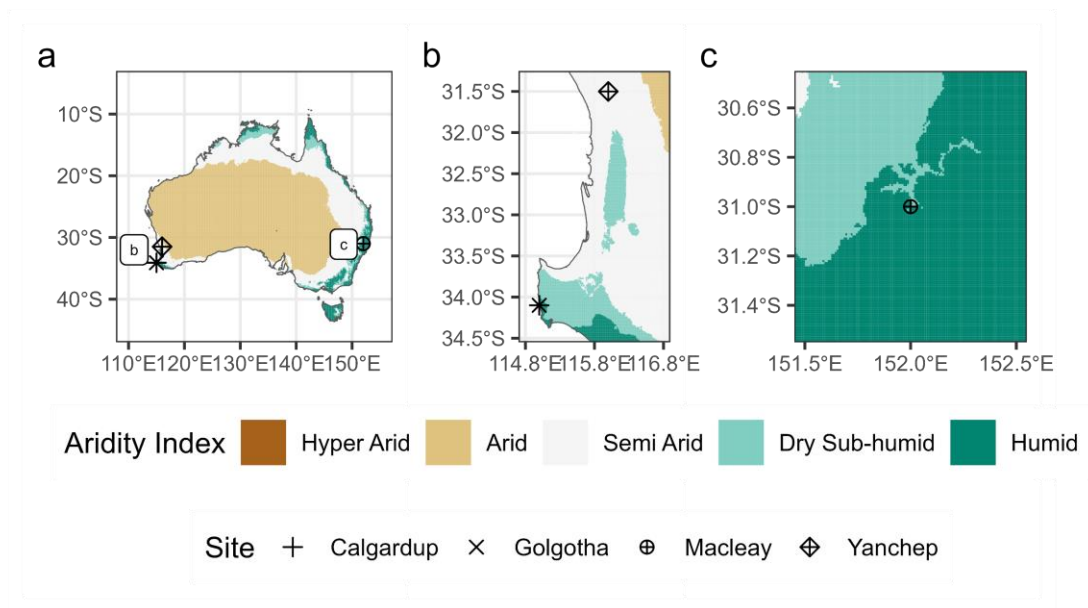


Figure 1 Map of Australia showing the four ash collection locations. Aridity Index is also mapped, according to Zomer et al., (2022). a) Australia, with collection sites indicated. b) southwest WA, with collection sites at Yanchep, Calgardup Caves, and Golgotha Cave indicated. c) the Macleay region, with collection site indicated. The base Australia map is the GEODATA TOPO 250K Series 3 (Geoscience Australia, 2006).

Both ash and soil samples were collected from above the Calgardup and Golgotha caves in the Capes region of southwestern Western Australia, between Cape Leeuwin and Cape Naturaliste (Figure 1). As for Yanchep, the underlying geology is Tamala Limestone, and the climate is also Mediterranean, although annual precipitation is higher and temperatures are more moderate than Yanchep. The vegetation community at Golgotha Cave is eucalypt open forest characterized by a mixed canopy of marri (*E. calophylla*) and jarrah (*E. marginata*) with occasional karri (*E. diversicolor*) on the ridge above the cave, and tall open karri forest below the cave. The understorey is a mix of *Agonis flexuosa*, *Trymalium spathulatum*, *Podocarpus drouynianus*, *Xanthorrhoea preissi*, *Bossiaea disticha* and *Templetonia retusa* (Treble et al., 2016). The Golgotha Cave ash samples were collected in January 2022, following a wildfire in December 2021 which burned nearly 8000 ha in the Leeuwin-Naturaliste National Park (DBCA-060 Fire History database; <https://catalogue.data.wa.gov.au/dataset/dbca-fire-history>). Of those ~8000 ha, ~5400 ha are classified by dNBR as being of ‘High Severity’ (dNBR > 0.66; Key and Benson, 2006), and ~1400 ha classified as ‘Moderate-high severity’ (dNBR between 0.44 and 0.659; Key and Benson, 2006). See Text S1 for a dNBR map of this event.

Dominant vegetation at Calgardup Cave is low open forest of jarrah and marri with a dense and diverse understorey comprised mainly of *Banksia*, *Xanthorrhoea*, *Hakea*, and *Melaleuca* species close to the cave entrance, but which grades into a mix of marri-jarrah and karri to the southwest. The Calgardup Cave ash samples were collected in August 2018 one day after a low-intensity prescribed burn. The fire was small, highly localised, and cloud cover too heavy for dNBR analysis of this event. However, post fire condition showed that no canopy was burnt and that severity was overall low. Soil samples were collected opportunistically from above both the Calgardup and Golgotha caves, and from six other sites in the Leeuwin-Naturaliste National Park between 2006 and 2022.

2.1.2 Southeast Australia

Ashes were collected from the Macleay Karst Arc, located in the Mid North Coast of New South Wales (NSW), southeast Australia (Figure 1). The underlying geology is a Permian limestone, comprised of a basal calcareous mudstone, a central unit of crinoidal limestone, and discontinuous reef limestones (NSW Department of Environment, Climate Change and Water, 2011). The climate is temperate humid sub-tropical, with strong temperature seasonality, and a seasonal bias in precipitation with most precipitation occurring in summer (Baker et al., 2020). Vegetation is varied, with some subtropical rainforest, interspersed with cleared areas. Ash samples were collected in February 2020 following the Carrai East fire, which burned from October 2019 to January 2020 during the Australian 'Black Summer' fire season. The fire burned ~150278 ha (NSW Rural Fire Service, 2020). dNBR analyses suggest that this includes ~42000 ha burned at high severity, and ~75000 ha at moderate-high severity, noting that the unusual length of the event (two months) may have skewed dNBR results (see Text S1).

No soil samples were collected from southeast Australia, as the site was not accessible due to extensive flood damage in 2022 following the fires in 2019/2020.

2.2 Fire histories

Fire histories for each site were extracted from databases. The Western Australian Department of Biodiversity, Conservation, and Attractions (DBCA) maintains a spatial dataset of known fires in Western Australia (DBCA-060 Fire History), with fire event polygons, fire type, fire size, and approximate dates, among other fields (<https://catalogue.data.wa.gov.au/dataset/dbca-fire-history>, accessed November 2022). The earliest fires recorded in the database are from 1937, and known issues include missing events and inaccurate dating (Dixon et al., 2022). The New South Wales National Parks and Wildlife Service (NPWS) maintains a dataset of wildfire and prescribed burn events which occurred within the NPWS estate, as well as some fire events which occur or extend beyond the estate (NPWS Fire History – Wildfires and Prescribed Burns; <https://datasets.seed.nsw.gov.au/dataset/fire-history-wildfires-and-prescribed-burns-1e8b6>, accessed in November 2022). The database includes fields which describe the fire extent and type of fires which have occurred since 1920, and was last revised in October 2022.

The two fire history databases were interrogated using *QGIS* (3.28.0) and *R* (version 4.3.1), with the *dplyr* (1.1.2), *sf* (1.0.14), and *rgdal* (1.6.7) packages (Bivand et al., 2021; Pebesma, 2018; QGIS Development Team, 2022; R Core Team, 2023; Wickham et al., 2020)), and fire histories for each ash and soil sampling location were extracted. Scripts detailing this process are available in the supplementary dataset (Campbell et al., 2024). These fire histories are represented in the dataset as two variables – the number of years since the last fire prior to collection (i.e. the penultimate fire for ash samples), and the total number of fires experienced for each sample location. Some manual corrections were made to the fire histories where the spatial resolution of the database was sufficient to accurately delineate between burned and unburned sites at the fire edge. Where the location had not experienced a fire during the observational period (i.e. 8 of the 9 Macleay samples), the years since last fire was given as 100 years, the length of the NPWS database.

For the length of the fire history databases, most sample sites had experienced at least one fire during the observational period, with a median number of fires of four and a maximum of nine. Of the sampling sites, Macleay sites had had the fewest total fires, Yanchep sites had experienced between three and nine fires, Golgotha Cave experienced between four and five fires, and Calgardup Cave had five recorded fires.

The median period since the last fire for all sample locations was 14 years, and 88% of sample locations had burned in the 50 years prior to collection. For the ash samples, sample sites above Calgardup Cave and at Yanchep had burned most recently (years since previous fire were 10 and 14 years, respectively). Sample locations above Golgotha Cave sample locations were last burned 16 years before sample collection. Most Macleay sample locations had no recorded fires, but one sample location had burned 18 years prior to sample collection.

2.3 Sampling protocols

Forty-three ash samples were opportunistically collected following fire events at the sites described above. Ash samples were collected one day after fire at Calgardup Cave, ~1 month post-fire at Golgotha Cave and Yanchep National Park, and within maximum three months of the fire at Macleay. Ashes were classified according to a simple colour classification: black, grey, red, and white (Figure 2). Ash sampling was targeted for inorganic analyses in the first instance. Plastic equipment was used to collect and store the samples to avoid contamination with metals. At Golgotha Cave (the most recent site sampled), a duplicate dataset was collected specifically for organic geochemistry analyses. These samples were collected using metal implements and stored in aluminium foil to minimise plastic contamination. A limited number of samples from Yanchep, Calgardup Cave, and Macleay which were collected with the inorganic sampling protocol were subsequently also analysed for lipid biomarkers. Samples collected for inorganic analyses were stored in plastic zip loc bags in a cool storage room. Samples collected for organic analyses were stored in aluminium foil in a cool storage room.

Ash samples are not evenly distributed by either site or ash colour. A greater number of samples were collected at Yanchep, with the fewest samples collected at Calgardup Cave (Figure 2). More grey and black samples ($n = 17$ and $n = 16$, respectively) were collected than red and white samples ($n = 1$ and $n = 9$; Figure 2). This is due to the opportunistic nature of sampling, which largely relied on volunteer efforts.

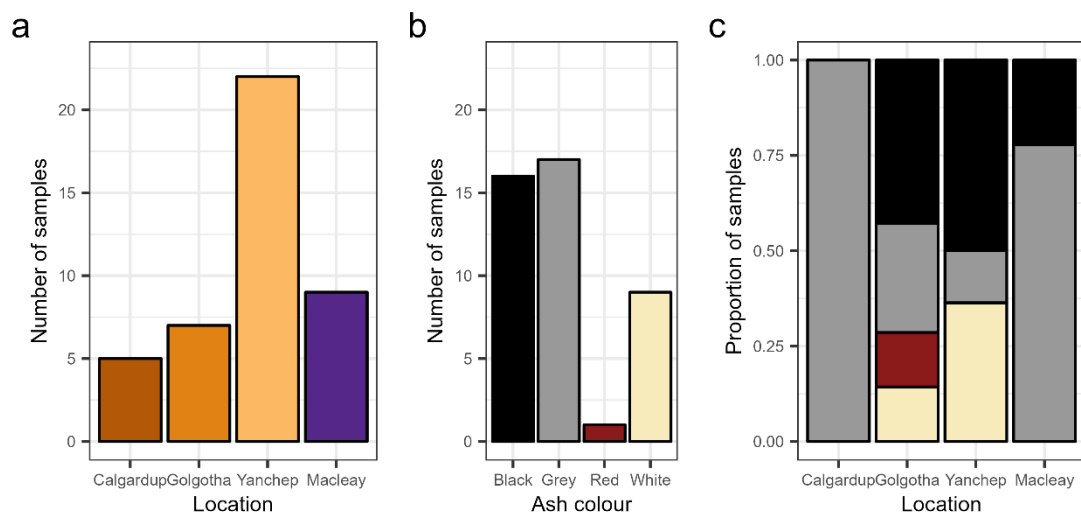


Figure 2 The distribution of ash samples by location (a), ash colour (b), and both location and ash colour (c).

A total of 44 soil samples were collected from ten sites in southwest Australia in 2006, 2015, and 2022. The 2006 and 2015 sampling targeted the Capes region sites, while 2022 sampling targeted both the Capes region and Yanchep National Park (see Table S1 for a list of soil sampling locations). The 2006 samples collected from Golgotha Cave were collected as part of sample collection for Treble et al. (2016), while 2015 Capes region samples were targeted at sites that had experienced recent fire (e.g. Moondyne in 2003) and sites which had not burned in decades (e.g. Jewel Cave which last burned in 1961). 2022 sampling was undertaken on sites which had burned in recent years at both Yanchep and in the Capes region, some of which had previously been sampled in 2006 and/or 2015. Sampling protocol was to collect soil at depths of 0-10 cm, and 10-20 cm (for one sample only the top 5 cm of soil was collected). For statistical analyses, all samples are categorised as sampled from 0-10 cm or 10-20 cm. Samples were not evenly selected by site or location, with a larger number of samples collected from the Capes region than from Yanchep. More than 20% of samples were collected at Golgotha Cave.

2.4 Inorganic analyses

Inorganic geochemistry was undertaken on all ash and soil samples at the Isotope Tracing in Natural Systems laboratory at ANSTO, Lucas Heights, Australia. Ash leachates were extracted from unhomogenised samples using the USGS field leach test (Hageman, 2007). Sample was mixed with deionised water at a ratio of 1:20 by weight, agitated for 15 minutes, and then rested for 10 minutes. The supernatant was filtered using 0.45 µm pore-size nitrocellulose filters and alkalinity and pH measurements were performed using a Metrohm 862 Compact Titrator following Standard Methods for the Examination of Water and Wastewater, Method 4500-CO₂ D. Carbon Dioxide and Forms of Alkalinity by Calculation (American Public Health Association, American Water Works Association, Water Environment Federation et al., 2017). Electrical conductivity (EC) for a subset of samples was measured by Radiometer CDM92 conductivity meter. A sub-sample was acidified with Merck Suprapur HNO₃ to 1% (vol/vol) for cation analysis by inductively coupled plasma atomic emission spectroscopy (ICP-AES) and inductively coupled plasma mass spectrometry (ICP-MS), and an unacidified portion retained for anion measurement by ion chromatography (IC). Samples were stored in laboratory refrigeration at 4 °C prior to analysis. To analyse a majority of (including volatile) elements, soil leachates were prepared as received to maintain their integrity. One batch of samples (2022/0199) were subsequently corrected for moisture content for report consistency with the other samples, as they were moist when collected – see Text S2 for correction equations.

The charge balance error (%) was calculated for ash and soil leachates in PHREEQC. For ash leachates, total alkalinity, pH, Ca, K, Mg, Na, Si, P, Sr, Ba, Br, F, Cl, SO₄ and NO₃ were used as the input variables, with a temperature of 25 °C. Forty-three of the 58 samples (including replicates) returned charge balance errors within ±10%, while 23 samples returned charge balance errors within ±5% (noting that the charge balance was calculated on replicates separately; see Table S2 and Figure S1 for charge balance errors). The largest proportion of leachates with a positive charge imbalance were from black ashes (~47% of black ash samples >+10 % error), while only one grey ash leachate sample, and no white or red samples had a charge balance error >+10%. The positive charge imbalance for the black ash samples may be attributed to the higher proportion of organic matter typically found in black ashes (Bodí et al., 2014), which may have resulted in higher dissolved organic carbon concentrations in the leachates. This can result in organic anions contributing significantly to the charge balance. This is not accounted for in the PHREEQC charge balance calculation, which includes only inorganic ions (Dasgupta et al., 2015). Three ash leachates returned charge balance errors < -10%, two of which were <-40%. All three negatively charged

leachates were samples from the Macleay region. Most Macleay samples had charge balance errors < -5% (see Table S2).

Charge balance error was calculated for only 27 of 63 soil leachates (including replicates), due to missing pH data. For soil leachates, the input variables were total alkalinity, pH, Ca, Fe, K, Mg, Na, P, Br, Ba, Sr, Cl, SO₄, and NO₃, with a temperature of 25 °C. Twenty-two of the 27 samples returned a charge balance error within ±10%, and 11/27 returned a charge balance error within ±5% (see Table S3). One sample, collected at Yonderup, returned a charge balance error of ~+39%. Due to the small sample size, and uncertainty around the charge balance of the samples which could not be calculated using PHREEQC, no data were excluded from the subsequent statistical analyses.

Preliminary analysis of a subset of the ash data (nine variables measured in 16 samples from Yanchep National Park) was previously presented as a case study in Campbell et al. (2023). Results presented there showed that the ash leachate chemistry differed between black and white ashes (n = 16). This supported the hypothesis of McDonough et al. (2022) that speleothem palaeofire trace element proxies are sourced from ash.

2.5 Biomarker analyses

Biomass burning biomarkers (levoglucosan and PAHs) were analysed in the GNS/VUW Organic Geochemistry Laboratory at GNS Science, New Zealand. Freeze-dried, homogenised ash (0.33–0.95 g) samples were extracted three times with dichloromethane/methanol (3:1, v:v) by ultrasonication for 20 min each time, followed by centrifugation at 2000 rpm for 5 min. The resulting extracts were filtered on cotton wool-plugged Pasteur pipettes and evaporated under N₂ at 35 °C to obtain dried total lipid extracts (TLEs). Half of each TLE was derivatized with 50 µL *N,O*-bis(trimethylsilyl)trifluoroacetamide (BSTFA) with 1% trimethylchlorosilane (TMCS) at 70 °C for 1h. After cooling, the solutions were evaporated under N₂ at 35 °C until dryness and redissolved in *n*-hexane for analysis.

The derivatised TLEs were analysed by gas chromatography mass spectrometry (GC-MS) on an Agilent 7890A GC System, equipped with an Agilent J&W DB-5ms capillary column [60 m × 0.25 mm inner diameter (i.d.) × 0.25 µm film thickness (f.t.)], and coupled through a split to an Agilent 5975C inert MSD mass spectrometer and a flame ionisation detector (FID). The temperature programme of the oven was 70 °C to 130 °C at 20 °C min⁻¹, then at 4 °C min⁻¹ to 320 °C and held isothermal for 15 minutes, which results in a total run time of 65.5 min. Helium was used as carrier gas with a constant flow of 1.0 mL min⁻¹. Samples (3 µL) were injected splitless at an inlet temperature of 300 °C. The MS was operated in electron impact ionisation mode at 70 eV using a source temperature of 230 °C. After a solvent delay of 10 min, samples were analysed in full scan mode with *m/z* 50–700.

Internal standards (5 α -cholestane, *n*-nonadecanol and *n*-nonadecanoic acid) for quantification were added to the samples prior to the first extraction. Procedural blanks and laboratory reference standards were also analysed to ensure data quality and absence of laboratory contaminants.

Analyses of Golgotha Cave ash samples were repeated in November 2023 to test for alteration of the biomarker signal *ex situ*. The same sample protocol as above was followed, except larger sample sizes (up to 2.81 g) were used.

2.6 Software and statistical methods

Data were analysed and visualized using the statistical software *R* (version 4.3.1), and the packages *readr* (2.1.4), *dplyr* (1.1.2), *ggplot2* (3.4.2), *boot* (1.3-28.1), *ShapleyValue* (0.2.0), *stringr* (1.5.0), *tidyr* (1.3.0), *ggbiplot* (0.55), *EnvStats* (2.8.0), *purrr* (1.0.1), and *stats* (4.3.1) (Canty and Ripley, 2022; Davison and Hinkley, 1997; Liang, 2021; Millard, 2013; R

Core Team, 2023; Vu, 2011; Wickham, 2022, 2016; Wickham et al., 2023, 2020; Wickham and Henry, 2023). Fire history databases were clipped to the study sites in QGIS (3.28.0) before interrogation in R (QGIS Development Team, 2022). Figure 3 shows the data processing workflow and the analytes used for each statistical test.

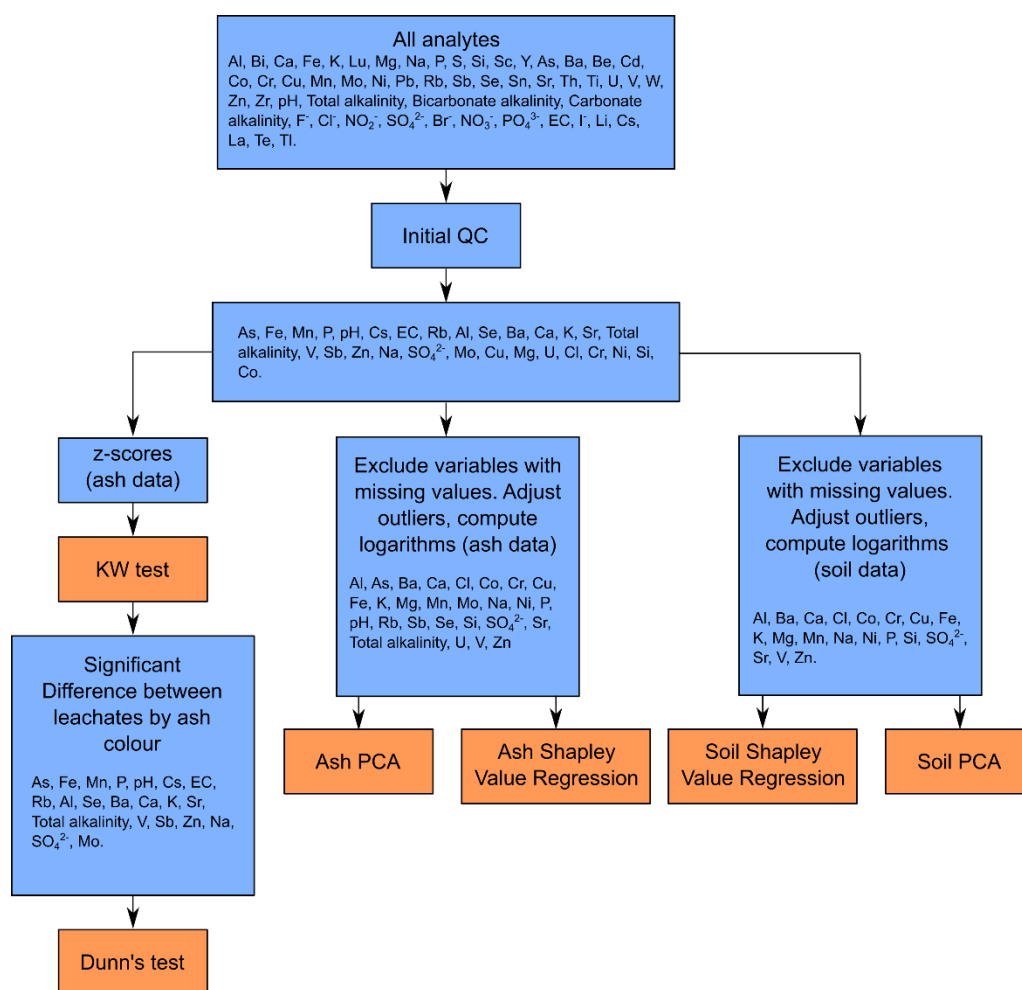


Figure 3 the workflow for the data processing and statistical analyses of inorganic leachate data. Orange boxes indicate a statistical test, blue boxes indicate a data processing step.

Where replicate leachates were analysed, the results were combined and the means used in the statistical analyses. Outliers in the soil and ash leachates chemistry were identified using Rosner's Test in the R package 'EnvStats', which allows for multiple outliers to be identified (Millard, 2013; Rosner, 1983). Outlier identification was adapted from a script presented in Croke et al. (2021). As the sample sizes for soil ($n = 43$) and ash ($n = 44$) leachates are small, outliers were replaced with the median value rather than removed. Histograms of the data distributions for both soil and ash leachates with outliers indicated are found in Figures S2 and S3. Histograms show that geochemistry data are all skewed, necessitating either transformation or non-parametric statistical tests. Initial quality control was conducted to limit the number of analytes included in the statistical analyses (see Text S3 for details).

To test how ash chemistry changes with ash colour, we applied the non-parametric Kruskal-Wallis rank sum test to determine if there was significant difference in ash chemistry between ash colours (Hollander and Wolfe, 1973). To minimise the impact of location on ash chemistry, data were first grouped by location and then transformed to z-scores. The null

hypothesis of the Kruskal-Wallis test is that samples originate from the same distribution, with the alternative hypothesis that the samples originate from different distributions. A significant Kruskal-Wallis result indicates that there is some difference in the distributions, but it cannot tell where that difference occurs. Dunn's Test is the nonparametric post-hoc test for multiple comparisons (Dunn, 1964), and shows which variables are significantly different from one another. The null hypothesis is that there is no difference between groups, while the alternative hypothesis is that there is a difference between groups. Importantly, Dunn's test allows for groups to be of equal or unequal size.

Shapley Value regression allows for the relative importance of predictor variables in linear regression to be calculated. It achieves this by computing the R-squared for each possible combination of predictor variables and calculating the average improvement when adding a variable to a model (Budescu, 1993; Lipovetsky and Conklin, 2001). Shapley value regression was undertaken on the ash and soil leachate data using the *ShapleyValue* package in *R* (Liang, 2021; R Core Team, 2023). For the ash samples, the predictors were ash colour, location, years since the last fire, and the total number of fires. For the soil sample analyses, the predictors were sample depth, location, years since the last fire, and the total number of fires. For both ash and soil data, values were log-transformed (base 10) prior to analyses. Confidence Intervals (CIs) were calculated at $\alpha = 0.95$ using the bias corrected and accelerated intervals (BCa) on bootstrap replicates of the standardised Shapley values ($R = 5000$). Bootstrap resampling and calculation of CIs were done using the *boot* package in *R* (Canty and Ripley, 2022; R Core Team, 2023). BCa intervals were used to calculate CIs as it is the only method which is guaranteed to return intervals within the statistics sampling space (0-1), and is in general recommended, given sufficient sample n and bootstrap replicates (Carpenter and Bithell, 2000; Puth et al., 2015)

Principal component analyses (PCA) were performed using the '*prcomp*' function in *R* on the logarithm (base 10) of the inorganic leachate data (R Core Team, 2023). The PCAs were done on the correlation matrix, and data were mean subtracted. Where zeroes were introduced due to how values less than the limit of detection were handled (by replacing those values with a random number between zero and the limit), these zeroes were replaced with the minimum measured value for that variable. Figures S2 and S3 show the distributions of the input data.

3 Results

3.1 Ash

3.1.1 Relationships between ash colour, chemistry and burn severity

We calculated the Ca/Mg ratio for each sample (Figure 4) and found that black ash leachates consistently have a Ca/Mg ratio greater than one (>80% of black ash samples), grey samples have a median Ca/Mg value of less than one, but 35% of samples had a ratio greater than one. While the median Ca/Mg value for white ash is slightly higher than that of grey ash (0.57 as opposed to 0.55 – with an outlier of > 30 000 removed from the white samples), but less variable ($\sigma = 0.266$ as opposed to $\sigma = 2.38$) and just two of nine white ash samples have a Ca/Mg value greater than one. The red ash leachate sample had a ratio comparable to that of black ash.

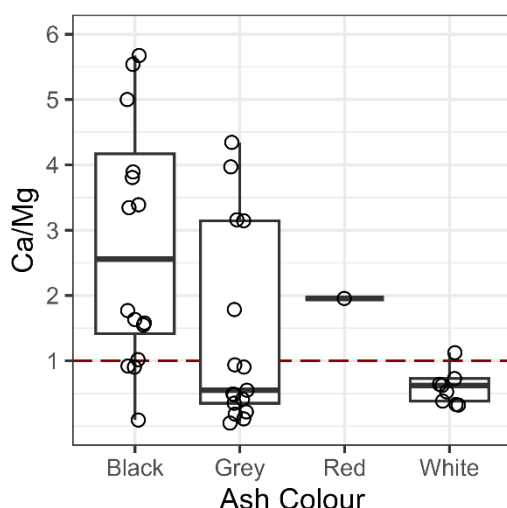


Figure 4 Boxplots of Ca/Mg ratios of ash leachates for all sites by ash colour. The dashed red line indicates a Ca/Mg ratio of 1. Note that two outliers are omitted from this plot by the y-axis scaling - one black ash sample with a Ca/Mg value of 11.8, one grey ash sample with a Ca/Mg of ~9.2, and one white ash sample with a value of 34067.8, due to very low Mg concentration in that sample.

Ash leachate chemistry has been shown to vary with ash colour, which is itself a product of combustion completeness. Here, we tested for significant difference in ash leachate chemistry between ash colours using both the Kruskal-Wallis ranked sum test and Dunn's test, which makes multiple pairwise comparisons. The results of the Kruskal-Wallis test showed that there is a significant difference in the pH, total alkalinity, EC, Na, K, Rb, Cs, Al, Mn, Fe, P, As, Se, and SO_4 (see Table S4 for Kruskal-Wallis p-values). Dunn's test for multiple comparisons show which ash colour groups are statistically different from one another. Figure 5 shows boxplots of the z-scores of each variable by ash colour. The results of Dunn's test are labelled, showing that in general it is only the severity end members (black and white ashes) which report significantly different concentrations. Boxplots of all variables by ash colour are found in Figure S4, and a table of mean non-normalised values for each variable is presented in Table S5.

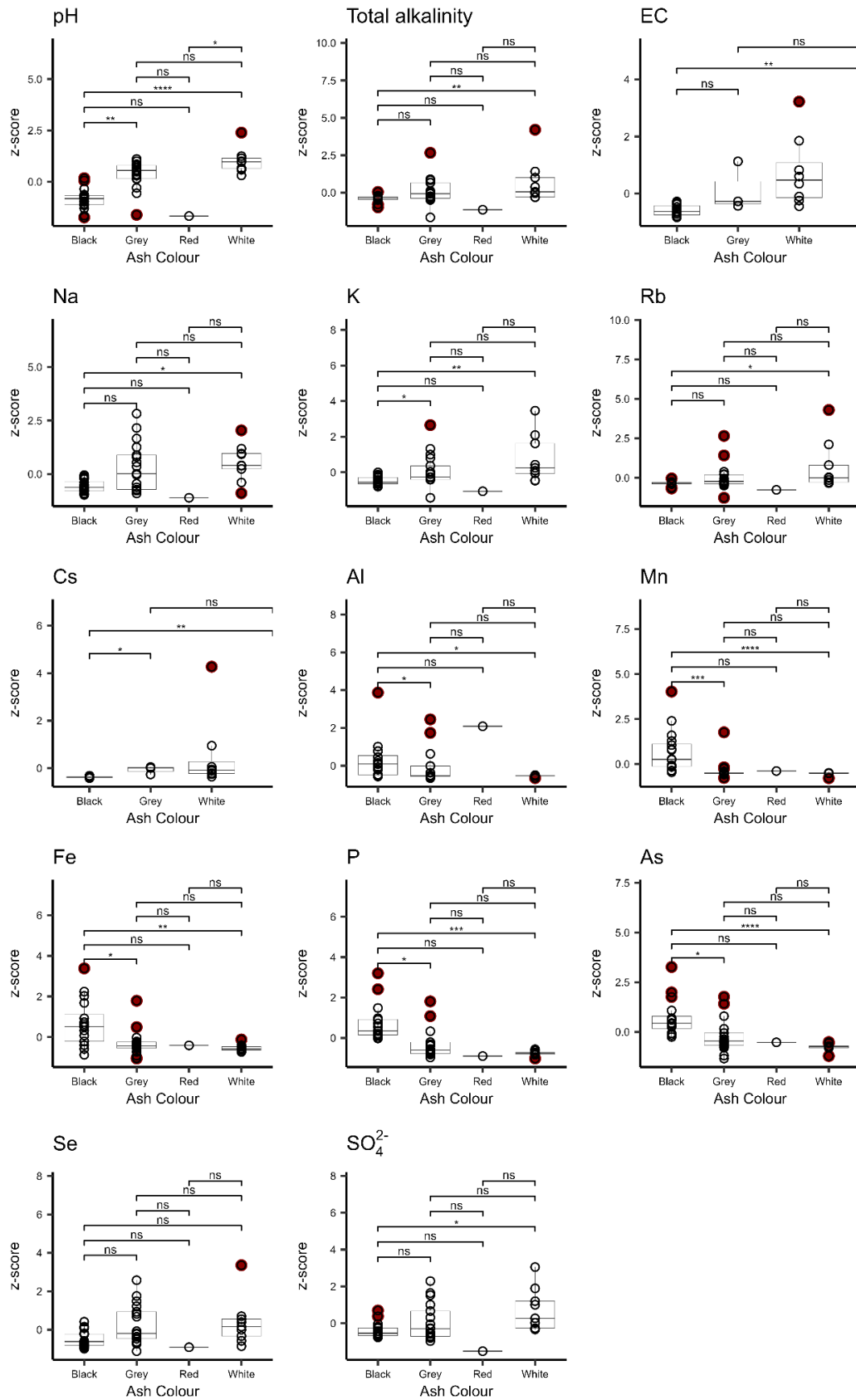


Figure 5 Boxplots showing z-scores of ash leachate elemental concentrations, electrical conductivity, pH, and alkalinity. The results of Dunn's test are also indicated. *

indicates significance at $\alpha = 0.05$, ** significant at $\alpha = 0.01$, *** significant at $\alpha = 0.001$,
**** significant at $\alpha = 0.0001$. Red points indicate outliers.

Where black and white ash leachate analytes were significantly different (pH, total alkalinity, EC, Na, K, Rb, Cs, Al, Mn, Fe, P, As, and SO_4), values were higher in black than white ash leachates for Al, Mn, Fe, P, and As, while values were higher in white than black ash leachates for total alkalinity, pH, EC, Na, K, Rb, Cs, and SO_4 . Despite the Kruskal-Wallis test indicating that concentrations of Se were significantly different between different coloured ashes (Table S4), Dunn's Test found that the chemistry of the black, grey, and white ash leachates were statistically similar for these analytes. While in general the differences between the end members (black and white ash) were the most significant, grey and black ashes were significantly different for pH, K, Cs, Al, Mn, Fe, P, and As. There is no evidence of statistical differences between grey and white ashes (Figure 5).

3.1.2 Predictors of ash leachate chemistry

Shapley value regression is used to quantify the influence of predictor variables (see section 2.6). Standardized Shapley regression values were calculated for each of the 27 ash leachate variables and four predictors (ash colour, location, year since the last fire, and the total number of fires), with 95% CIs. Results show that ash colour was the most important predictor for 11 variables (Al, As, Fe, K, Mn, Mo, Ni, P, pH, Rb, and Zn), location was the most influential predictor for 16 variables (Ba, Ca, Cl, Co, Cr, Cu, Mg, Na, Sb, Se, Si, SO_4 , Sr, total alkalinity, U, and V). Ash colour was the dominant predictor (standardized Shapley value >0.5) for Al, As, Mn, Mo, P, and pH. Location was the dominant predictor for Ba, Ca, Cu, Sb, Se, Si, Sr, U, and V. Neither years since the last fire nor the total number of fires were the dominant predictor for any variables. The highest standardised Shapley value for years since last fire and the total number of fires were 0.288 (Cr) and 0.319 (Mg), although these values were associated with wide CIs (see Table S6 and Figure S5). There is also a high overlap in the 95% CIs for each predictor for many variables, particularly for ash colour and location.

PCA was applied to the full ash leachate dataset (Al, As, Ba, Ca, Cl, Co, Cr, Cu, Fe, K, Mg, Mn, Mo, Na, Ni, P, pH, Rb, Sb, Se, Si, SO_4 , Sr, total alkalinity, U, V, and Zn (Table 1)). A scree plot (see Figure S6) suggests that while the first three principal components (PCs) contain the most information, the first seven PCs each contain more information than if all PCs explained an equal amount of variance, and so should also be presented. Together the first two PCs account for ~45% of the variance, and >95% of the variance is described by the first 15 PCs. Loadings can be considered to be important if they contribute more than the average amount of information to the PC. Here, that threshold is ± 0.192 .

Table 1 presents the loadings for the first seven PCs. Loadings and a biplot of PC1 and PC2 (Figure 6a) shows that black ash samples cluster differently to white and grey ash samples. Variables which load strongly positively on PC1 (Al, Mn) all have higher concentrations in black ash than white ash, while variables which load strongly negatively on PC1 (Cl, Cr, K, Na, pH, SO_4 , Rb, and total alkalinity) are all higher in white ash than black ash, noting that the difference between white and black leachates is not statistically significant for Cl and Cr (Figure 5, Figure S4). The clustering of grey/white versus black ash leachates suggests that burn severity impacts ash leachate geochemistry.

564 **Table 1 Loadings for the first seven PCs from the PCA of ash leachate data. Variables**
565 **which explain more than one variable's worth of information to the PC (threshold =**
566 **0.19) are in bold.**

| | PC1 | PC2 | PC3 | PC4 | PC5 | PC6 | PC7 |
|-----------------------------------|---------------|---------------|---------------|---------------|---------------|---------------|---------------|
| Al | 0.218 | -0.147 | 0.162 | -0.115 | 0.089 | -0.291 | 0.194 |
| As | 0.185 | -0.231 | 0.272 | -0.036 | 0.092 | -0.184 | -0.141 |
| Ba | -0.050 | -0.388 | -0.214 | 0.087 | -0.026 | 0.124 | -0.006 |
| Ca | 0.048 | -0.319 | -0.172 | 0.091 | -0.134 | 0.427 | -0.162 |
| Cl | -0.290 | -0.135 | 0.056 | -0.109 | 0.188 | -0.022 | 0.052 |
| Co | 0.084 | -0.103 | 0.264 | 0.150 | -0.416 | 0.154 | -0.016 |
| Cr | -0.242 | -0.024 | 0.026 | -0.281 | -0.168 | -0.237 | 0.009 |
| Cu | 0.063 | 0.105 | 0.208 | -0.043 | -0.363 | 0.305 | 0.457 |
| Fe | 0.148 | -0.121 | -0.214 | -0.231 | 0.106 | 0.227 | 0.484 |
| K | -0.311 | -0.062 | 0.079 | -0.113 | 0.047 | 0.040 | -0.045 |
| Mg | -0.161 | -0.185 | 0.185 | 0.054 | 0.342 | 0.240 | 0.262 |
| Mn | 0.250 | -0.155 | 0.137 | -0.253 | -0.070 | -0.171 | 0.010 |
| Mo | -0.174 | 0.109 | 0.212 | -0.033 | -0.365 | -0.061 | -0.166 |
| Na | -0.302 | -0.112 | 0.022 | -0.113 | 0.111 | -0.065 | 0.088 |
| Ni | 0.046 | -0.055 | 0.409 | -0.188 | -0.055 | 0.296 | -0.064 |
| P | 0.181 | -0.227 | 0.295 | -0.203 | 0.061 | -0.147 | 0.126 |
| pH | -0.226 | 0.271 | -0.076 | 0.067 | -0.176 | -0.137 | 0.147 |
| Rb | -0.319 | -0.063 | 0.016 | -0.107 | -0.035 | -0.038 | 0.067 |
| Sb | -0.096 | 0.051 | 0.371 | 0.258 | 0.144 | 0.254 | -0.090 |
| Se | -0.104 | 0.305 | 0.198 | -0.006 | 0.233 | 0.172 | -0.137 |
| Si | -0.055 | -0.199 | 0.125 | 0.429 | -0.076 | -0.108 | -0.034 |
| SO ₄ | -0.298 | -0.114 | 0.022 | -0.183 | -0.036 | 0.092 | 0.009 |
| Sr | -0.096 | -0.390 | -0.205 | 0.072 | -0.029 | 0.053 | -0.179 |
| Total alkalinity | -0.302 | -0.036 | 0.064 | -0.128 | -0.022 | 0.001 | 0.109 |
| U | -0.149 | -0.269 | 0.021 | 0.095 | -0.369 | -0.220 | 0.102 |
| V | -0.086 | -0.126 | 0.225 | 0.406 | 0.234 | -0.248 | 0.145 |
| Zn | 0.025 | -0.093 | 0.086 | -0.368 | 0.050 | 0.080 | -0.463 |
| Cumulative proportion of variance | 0.29 | 0.45 | 0.58 | 0.65 | 0.72 | 0.77 | 0.81 |

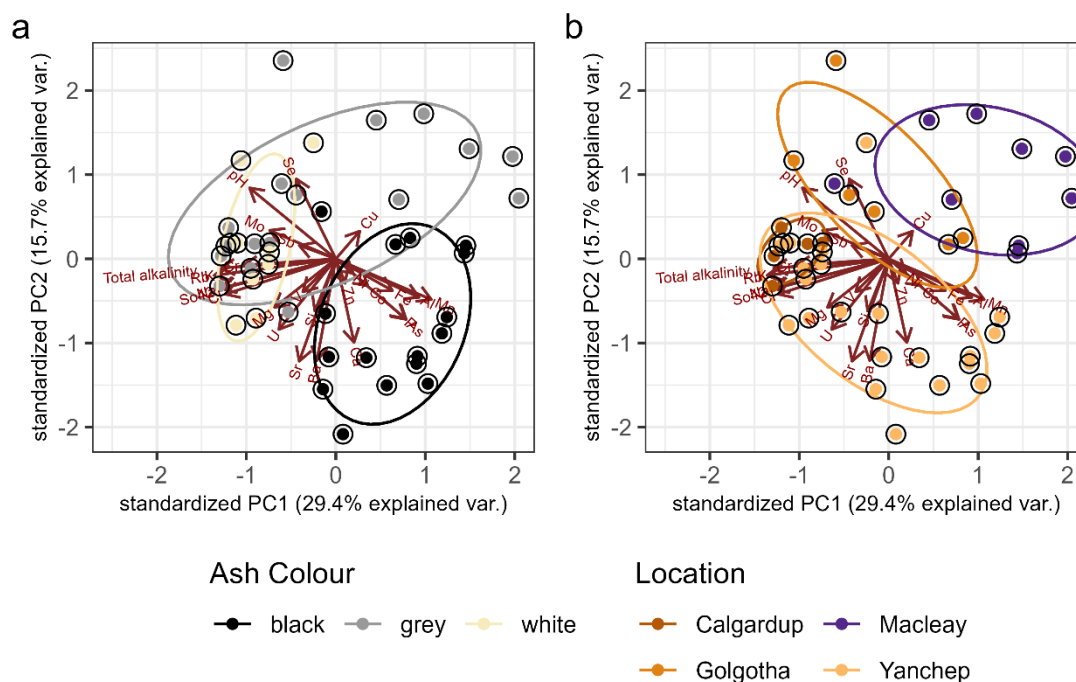


Figure 6 Biplots of standardised scores from PCA of ash leachate samples. 6a presents PC1 plotted against PC2, with ash colour shown as both clusters and the point colour. 6b also shows PC1 plotted against PC2, with sample location indicated by point colour and clustering.

Similarly, there is clear clustering of points by location, with samples from southwest western Australia and samples from southeastern Australia having little overlap in a biplot of PC1 and PC2 scores (Figure 6b), although it should be noted that the majority of Macleay samples were grey ashes. When samples are grouped by the number of years since the last fire (two groupings applied: samples below the median (14 years) or equal to and above the median), the samples clearly cluster, with sites burned less recently having more negative scores for PC2, while sites which burned more recently having more positive PC2 scores (see Figure S7). Biplots of the first three PCs for the total number of fires shows no distinct clustering (see Figure S8).

3.1.3 Ash biomarkers

Thirteen samples from four locations (Golgotha Cave, Calgardup Cave, Macleay, and Yanchep) were analysed, with six PAHs (Phenanthrene, Anthracene, Pyrene, Chrysene, Benzantracene, and Benzopyrene) and levoglucosan detected. Samples from Calgardup Cave and Macleay had no measurable PAHs or levoglucosan, and samples from Yanchep had no measurable PAHs, and concentrations of levoglucosan were low (see Table S7). As such, only ash samples from Golgotha Cave are presented here. Concentrations are normalised to the dry weight of ash.

In general, total concentrations of the low molecular weight compounds (Anthracene, Phenanthrene, and Pyrene) were higher than for higher molecular weight PAHs (Chrysene, Bezantracene, and Benzopyrene). PAH concentrations were generally higher in black and grey than white ash samples, particularly in the lowest molecular weight compounds, noting however that the variability for the black ash leachates is high for each PAH (Figure 7 and

Table S7), and that one black sample (Golgotha_6) had no measurable PAHs (Table S7). No PAHs were found in the red ash sample.

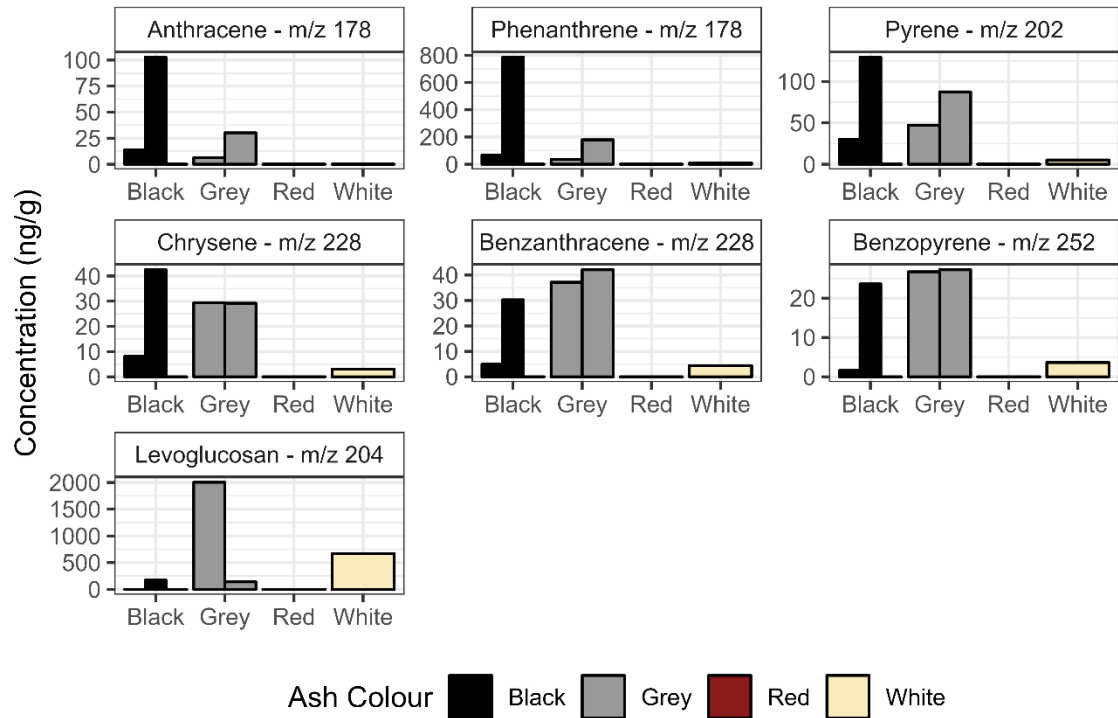


Figure 7 Concentrations of PAHs and levoglucosan, by ash colour. PAHs are arranged by molecular weight. Note that the scale of the y-axis is different for each plot.

Levoglucosan had a maximum concentration of 2.0 $\mu\text{g/g}$, and a mean concentration of 4.3 $\mu\text{g/g}$ (Figure 7, Table S7). Three (two black and one red) of the seven ash samples contained no measurable levoglucosan (see Table S7). Of the four Golgotha Cave samples with measurable concentrations, grey and white samples generally had higher concentrations than black samples (Figure 7).

3.2 Soil

Standardised Shapley regression values for 17 measured variables and four predictors (location, the number of years since the last fire, the total number of fires, and the sample depth) showed that location had the most explanatory power for all variables in soil leachates (see Table S8). There was no overlap in the 95% CIs between location and the other predictors for any analyte except Si, where CIs for depth, years since last fire, and total number of fires slightly overlapped with those for location (see Table S8 and Figure S9). This suggests that for most variables, sample location clearly has the greatest influence.

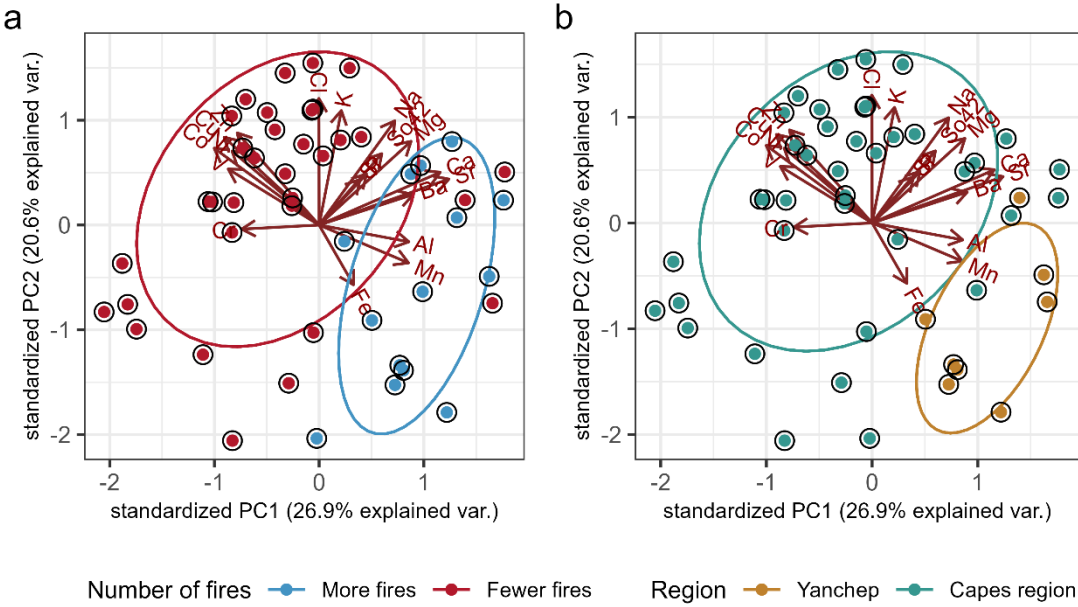
PCA was repeated on the soil leachates, using the same variables as for the PCA of ash leachates in Section 3.1, but with the exclusion of As, Mo, pH, Rb, Sb, Se, total alkalinity, and U due to missing data (Table 2). A scree plot (see Figure S10) suggests that while the first two PCs explain the most variance, the first five PCs each explain an above-average proportion of the variance, and should be presented. Together, the first two PCs explain ~48% of the variance, and >95% of the variance is explained by the first 13 PCs. Following Section 3.1, the threshold for loading 'importance' is ± 0.229 . Table 2 presents the loadings for the first five PCs. Variables which load strongly positively on PC1 (Al, Ba, Ca, Mg, Mn, Sr) are all variables which tend to be higher in the Yanchep region than the Capes region, and which

are higher at sites which have experienced more fires. Similarly, the variables which load strongly negatively on PC1 (Co, Cu, Ni, and V) are all lower for samples from the Yanchep region, and for samples which have experienced more fires. This is illustrated in a biplot of PC1 and PC2 (Figure 8).

Cl, Co, Cu, K, Mg, Na, Ni, and Zn load strongly positively on PC2, while no variable loads strongly negatively. A biplot of PC1 and PC2 with scores coloured by the distance to the coast (Figure 9) suggests that PC2 reflects proximity to the coast, with higher Cl, K, Mg, and Na in samples with higher exposure to sea spray (Davies and Crosbie, 2018).

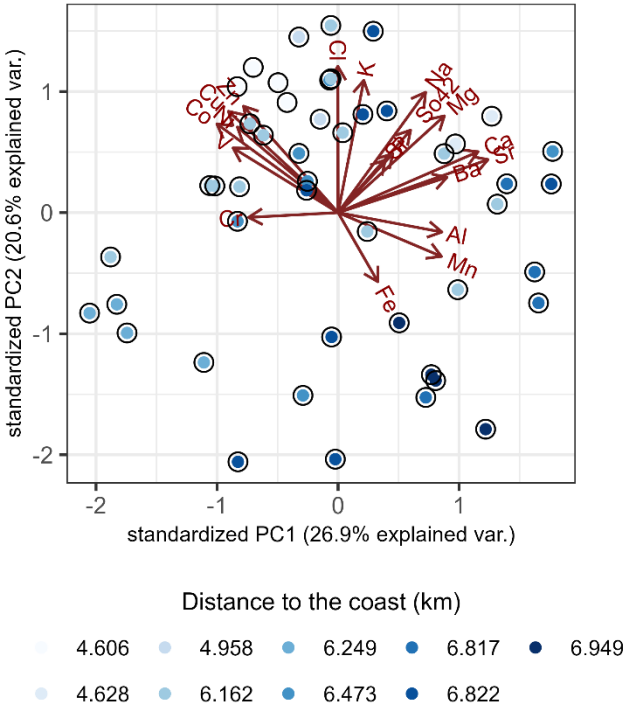
Table 2 Loadings for the first five PCs of soil leachate chemistry. Bold indicates which variables have a greater proportion of influence on the PC (threshold of ± 0.229)

| | PC1 | PC2 | PC3 | PC4 | PC5 |
|-----------------------------------|---------------|--------------|---------------|---------------|---------------|
| Al | 0.250 | -0.053 | -0.315 | -0.078 | -0.496 |
| Ba | 0.263 | 0.097 | 0.137 | 0.309 | -0.010 |
| Ca | 0.338 | 0.168 | 0.198 | 0.178 | -0.238 |
| Cl | -0.001 | 0.403 | -0.126 | -0.300 | 0.042 |
| Co | -0.292 | 0.245 | -0.130 | 0.086 | -0.080 |
| Cr | -0.216 | -0.013 | -0.396 | 0.044 | -0.407 |
| Cu | -0.265 | 0.279 | 0.071 | 0.079 | 0.039 |
| Fe | 0.096 | -0.190 | -0.512 | 0.123 | -0.145 |
| K | 0.062 | 0.365 | -0.355 | 0.061 | 0.118 |
| Mg | 0.256 | 0.267 | 0.017 | 0.235 | -0.224 |
| Mn | 0.249 | -0.121 | -0.238 | -0.054 | 0.333 |
| Na | 0.211 | 0.332 | -0.026 | -0.344 | 0.107 |
| Ni | -0.243 | 0.236 | 0.005 | 0.262 | 0.073 |
| P | 0.132 | 0.163 | -0.204 | 0.434 | 0.264 |
| Si | 0.114 | 0.145 | -0.301 | -0.010 | 0.389 |
| SO ₄ | 0.175 | 0.227 | 0.060 | -0.499 | -0.106 |
| Sr | 0.362 | 0.146 | 0.203 | 0.120 | -0.156 |
| V | -0.253 | 0.178 | -0.058 | -0.130 | -0.166 |
| Zn | -0.228 | 0.293 | 0.149 | 0.166 | -0.157 |
| Cumulative proportion of variance | 0.269 | 0.476 | 0.585 | 0.69 | 0.746 |



633

634 **Figure 8 A biplot of soil leachate PCA PC1 and PC2, with scores coloured by the**
635 **number of fires (a) and the region (b).**



636

637 **Figure 9 A biplot of soil PCA PC1 and PC2, with scores coloured by the distance from**
638 **sample location to the coast (in km)**

639 Figure 10 compares ash and soil leachate data for sites where both ashes and soils
640 were collected (Calgardup Cave, Golgotha Cave, and Yanchep). Ash leachates have higher

pH and alkalinity than soil leachates for all sites. Elemental concentrations are generally higher in ash leachates than soil leachates at two or more sites for all elements barring Fe, Al, and Cr. Concentrations of Fe are higher in soil leachates than in ash leachates at all sites. Concentrations of Al and Cr in soil leachates either exceed or are comparable to ash leachates (except for Calgardup Cave, where soil leachate Cr concentrations are very low). Concentrations of Na, K, Rb, Mg, Ca, Sr, Ni, Mo, P, Se, Cl, and SO₄ in ash leachates clearly exceed concentrations in soil leachates at all sites. Mn concentrations are generally higher in ash leachates at Golgotha Cave and Yanchep, but are comparable to soil leachates at Calgardup Cave. Concentrations of Ba, V, Co, Cu, Zn, Si, Sb, and U are higher in ash leachates than in soil leachates for Calgardup Cave and Yanchep samples, but are comparable in Golgotha Cave samples. A table of median soil leachate concentrations is found in Table S9. Concentrations of Al, Cl, Cr, and Fe were higher in leachates of deeper soils than in shallower soils (see Table S10).

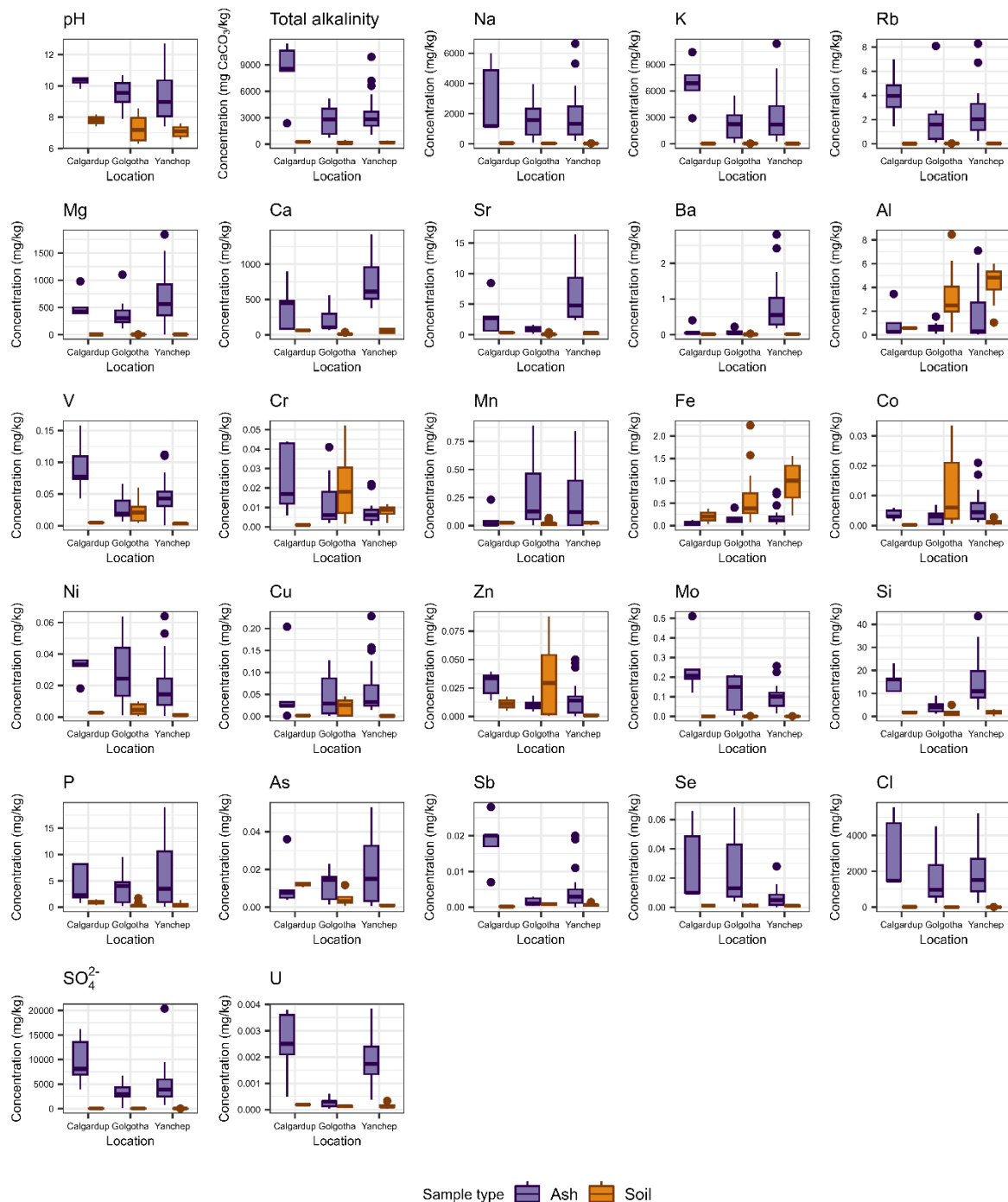


Figure 10 Boxplots of ash leachate (purple) and soil leachate (brown) chemistry for each site where both soils and ashes were collected (Calgardup Cave, Golgotha Cave, and Yanchep).

4 Discussion

Overall, our results shows that inorganic ash leachate chemistry varies with burn severity (as indicated by ash colour) and location, and that the past fire history (i.e., the total number of fires for each site, and the number of years since the last fire for each site), had a more limited effect on ash leachate chemistry. Ash leachate pyrogenic biomarker results were variable, and the relationship between ash colour and biomarker concentrations was not clear. Soil leachate chemistry was shown to vary between sites, and as for ash leachates, the fire

history had minimal impact on soil leachate chemistry. Ash leachates were generally shown to be more enriched in a range of analytes, compared to soil leachates.

4.1 Ash and soil leachate chemistry

4.1.1 General ash leachate chemistry

Of the 29 measured variables which met the threshold for inclusion ($\geq 25\%$ of samples $> \text{LOD}$), SO_4 , K, Cl, Na, and Ca were the most abundant elements in ash leachates, while U, Sb, Co, Cr, and Se were the least abundant elements. The elevated SO_4 , K, Cl, Na values in ash leachates are likely due to higher exposure of vegetation to sea spray, with all Western Australian ash samples collected within 8 km of the coast and downstream of the dominant southwesterly winds. This is also reflected in the soil leachate data, where PC2 reflected sea spray inputs and where the most abundant elements are Na, Cl, K, Ca, and SO_4 (Figure 10).

Our analyses of ash leachates from karstified limestone environments found Na to be the most abundant element, followed by Ca and Mg. These findings are broadly consistent with a recent global analysis of wildfire ash leachate data, which showed Na, Ca, and Mg to also be the most abundant ($\text{Ca} > \text{Na} > \text{Mg}$) (Sánchez-García et al., 2023). The predominance of Na in our samples again likely reflects the strong marine influence at our southwest Australian sites. The global analysis also showed that wildfire ash leachates were least abundant in F, Mn, and Fe, which is also in broad agreement with our results. Ash leachate concentrations presented here were generally higher than the ‘temperate eucalypt forest’ ash leachates from southeast Australian forests reported in Sánchez-García et al. (2023). However, Fe and Mn are an exception; our results show that these elements were both lower in concentration and outside the range of data presented by Sánchez-García et al. (2023).

4.1.2 Ash leachate chemistry changes with burn severity

Several studies have suggested that there is a relationship between combustion completeness and the Ca/Mg ratio, and a ratio < 1 is thought to indicate severe burning (Marion et al., 1991; Úbeda et al., 2009). Broadly, the results support the hypothesis that a Ca/Mg ratio < 1 indicates severe burning, particularly for the combustion end-members (black and white ash), but considerable spread in the data remains. This uncertainty is consistent with other studies. Úbeda et al. (2009) in a laboratory study of *Quercus suber* ash found that the relationship between the Ca/Mg ratio and combustion completeness only held for one site. While this ratio would require Ca concentrations to decrease with burn severity and Mg concentrations to increase with burn severity (or for one of these to not change with burn severity), the Kruskal-Wallis test found no statistical difference in the concentrations of these analytes between ash colours. However, a qualitative assessment of the data (see Figure S4) shows that in general, Ca concentrations are lower in white leachates than black ash leachates, while Mg concentrations are higher in white ash leachates. The lack of statistical difference between the concentrations of these analytes by combustion completeness is consistent with the literature, where they are generally reported to behave similarly (Balfour and Woods, 2013; Miotliński et al., 2023; Pereira et al., 2012; Úbeda et al., 2009), although Sánchez-García et al. (2023) reported that Ca concentrations were higher in ash leachates produced from severe burning, and that Mg concentrations did not vary with burn severity. The predominantly negative charge imbalances of the leachates also support the hypothesis that black ashes are less-combusted than white ashes. This was attributed to higher levels of organic matter in black ashes, which can contribute negative ions that are unaccounted for by our charge balance calculations.

Our hypothesis that ash leachate chemistry will change with burn severity, is supported by the Kruskal-Wallis rank sum test and post-hoc Dunn’s test, which showed that

pH, total alkalinity, EC, Cs, Rb, K, Na, and SO₄ increased with combustion completeness, while As, Fe, Mn, P, Al, and Zn decreased with combustion completeness. The Shapley value regression and PCA also indicated that ash colour (representing combustion completeness) is a key control on ash leachate chemistry. Note that in both Dunn's test and the PCA, there is little statistical difference between black and grey or grey and white ashes in any variable aside from K, where black ash leachates were significantly different from both grey and white ash leachates (Figure 6a). This suggests that it is only the severity end-members (more completely burned versus less completely burned) that can be distinguished in these analyses. We found no statistically significant difference in the water extractable proportion of Se, Ba, Ca, Sr, V, Sb, Mo, Cu, Mg, U, Cl, Cr, Ni, Si or Co by ash colour.

A comparison of our results with the literature is presented in Text S5. While a review of the literature broadly indicates that ash chemistry changes with burn severity, there is considerable heterogeneity of results, suggesting that there is a spatial and perhaps methodological influence on how ash geochemistry changes with burn severity. There is better agreement between studies of the water-extractable component of ash leachates (e.g. Burton et al., 2016; Miotliński et al., 2023; Pereira et al., 2012; Quintana et al., 2007; Sánchez-García et al., 2023; Úbeda et al., 2009), with acid-digested samples tending to be less consistent. In general, our results show strong agreement with Miotliński et al. (2023), for leachate data from combustion simulation experiments conducted on soils and vegetation litter from southwestern Western Australia, see Table S5.1 in Text S5.

If volatilization temperature was the sole control on element concentration with burn severity, we would expect to see concentrations of elements with high volatilization temperatures (e.g. Mn, Al, Zn, K, P, Cu, Mg, Ca and Na, which all volatilize at >700 °C (see summary figures in Campbell et al. (2023) and Bodí et al. (2014)) in greater relative proportions in white ashes than in black ash. This is true for Na and K which are higher in white ash leachates than in black ash leachates, but Mn, Al, P, and Zn are higher in black ash leachates than in white, and Cu, Mg, and Ca concentrations do not vary significantly with ash colour. Volatilisation temperatures reported in the literature are largely based on empirical combustion studies with varying experimental designs. Additional factors which may impact ash leachate chemistry beyond volatilisation temperature include combustion completeness (which can be independent of fire temperature), that the solubility of some metals changes with pH, and that some metals are likely to be present in complexes with organic matter (which is typically higher in incompletely combusted black ashes; Quill et al., 2010).

Levoglucosan is thought to form at burn temperatures between 150-350 °C (Kuo et al., 2008). Kuo et al. (2008) found that maximum levoglucosan yield in laboratory-produced black char occurred at 250 °C, and was independent of combustion duration. In results presented here, levoglucosan is highest in grey and white ashes, noting both the small sample sizes and that the spread of the grey data is high, and that while the highest concentration levoglucosan was found in a grey ash sample, the lowest non-zero concentration was also a grey ash sample. This may indicate that grey ash samples are heterogeneous. Alternatively, the difference between the two grey ash samples may be because levoglucosan production is independent of burn time (Kuo et al., 2008), and the grey sample with higher levoglucosan concentration may have been produced by long slow smouldering rather than hot fire.

Laboratory and field experiments have shown that low molecular weight PAHs tend to be more abundant in post-fire soils and burn residues after fires at low-to-moderate temperatures (Kim et al., 2011; Karp et al., 2020; Rey-Salgueiro et al., 2018; Simon et al., 2016), with lower concentrations found in laboratory residues at very low (<300 °C) and very high (>600 °C) temperatures (Karp et al., 2020). In wildfire ashes, summed PAHs have been

shown to be higher in black than in white ashes (Chen et al., 2018). In results presented here, PAH concentrations are generally higher in the lower molecular weight PAHs for all ash colours (Figure 7 and Table S7). Summed PAHs are also generally higher in black and grey ashes (see Figure S4.1 in Text S4), although there is significant variability in concentrations of the black ash samples (noting that only one each of red and white ashes are presented here). Higher concentrations of PAHs in black and grey ashes is to be expected, as at high temperatures PAHs may be completely combusted, or incorporated into larger aromatic compounds (Karp et al., 2020).

4.1.3 Ash and soil leachate chemistry varies among sites

Ash leachate chemistry varied between sites. Shapley value regression showed that for 16 variables (Ba, Ca, Cl, Co, Cr, Cu, Mg, Na, Sb, Se, Si, SO₄, Sr, total alkalinity, U, and V) location had more influence on ash leachate chemistry than ash colour. The second-most important predictor (above the threshold of 0.25, which indicates if a predictor explains more than its share of variance) was ash colour for Ba, Ca, Cl, Co, Cu, Na, Se, Si, SO₄, and total alkalinity. For Cr, years since the last fire was the second-most important predictor, while for Mg, the total number of fires was the second-most important predictor. The importance of location is also shown in the PCA, with ash leachates from different locations clustering differently, with the difference most obvious between southeast and southwest Australian samples. While there has been limited research on ashes from multiple sites, Úbeda et al. (2009) showed that in laboratory conditions, ash produced from *Quercus suber* from two different sites had distinctly different physical and chemical compositions. Sánchez-García et al. (2023) found that ashes from different sites clustered differently, although they attributed differences between the clusters to delays in sampling post-fire (with samples being rained on, or loss of the finer particles by wind) and to legacy contamination from industrial activity.

Time since sampling may have contributed to differences between Macleay ashes and the southwest Australian ashes, as the Macleay site was inaccessible due to the long duration of the Carrai East Fire. Approximately a month elapsed between the extinguishing of the fire in January 2020 and sampling in early February 2020, although due to the large size of the Carrai East Fire it is possible that the area that was sampled had extinguished much earlier than other parts of the fire. Both Golgotha Cave and Yanchep ashes were collected approximately one month after the respective wildfires, while Calgardup Cave ashes were collected one day after the prescribed burn.

Location was the most important predictor for soil leachates, as indicated by Shapley value regression and PCA results. Sub-plot-scale heterogeneity in soils has been well-documented (Campbell, 1979; Harris, 1915). The Shapley value regression showed that location was the dominant predictor for all variables. As for ash leachates, a standardised Shapley value >0.25 indicates that a predictor explains more than its share of variance if all predictors had equal predictive power. Unlike for ash leachate results, there are very few variables where the second-most important predictor exceeds this threshold (Cl and V), and for both variables the second-most important predictor was the total number of fires. Both PC1 and PC2 described some aspect of soil sample location, with PC1 perhaps conflating total number of fires and location, while elements which loaded strongly positively on PC2 were related to distance from the coast via sea spray inputs.

4.1.4 Limited evidence of memory of previous fires in ash and soil leachates

Neither the total number of fires nor the number of years since the last fire (both describing fire history) explained a large proportion of the variance in ash leachate chemistry, although PCA analysis of ash leachates showed that PC2 may describe the number of years

since the last fire, with sites which burned more recently loading positively on PC2, and sites which burned less recently loading negatively on PC2. Similarly, sites which had experienced more fires loaded positively on PC2, while sites which had experienced fewer fires loaded negatively on PC2, although the clustering is not as distinct as for the number of years since the last fire. This is reflected in the Shapley value regression, where the number of years since the last fire tends to be a more important predictor than the total number of fires (although less important than either ash colour or location). Shapley value regression showed that the number of years since the last fire had a sizable impact on Cr and SO₄ concentrations, while the total number of fires impacted Mg and Ni. This is consistent with Miotliński et al. (2023) who found higher concentrations in ashes produced from leaf litter and soil sampled from a site which had burned recently (2 months) than from a site burned less recently (4.5 years). That the effect appears to be tertiary to location and burn severity here may be explained by the much longer interval between the penultimate fire in results presented here.

As for ash leachates, neither the number of years since the last fire nor the total number of fires explained a large proportion of the variance in soil leachate chemistry, although PC1 may reflect the total number of fires (although this is potentially a confounding effect produced by correlation between location and the total number of fires, with Yanchep recording more fires than sites in the Capes region). Unlike for ash leachates, Shapley value regression of soil leachates suggests that the total number of fires has more impact on soil leachate chemistry than the number of years since the last fire, although only two variables (Cl and V) had standardised Shapley values >0.25.

4.2 Implications for palaeofire research

Past fire activity can be reconstructed using inorganic and organic proxies preserved in environmental archives such as soils, sediments, or ice cores. In recent years speleothems have been used to reconstruct past fire activity in Australia and North America (Argiriadis et al., 2019, 2023; Homann et al., 2023, 2022; McDonough et al., 2022). Fire sensitive stalagmite proxies include trace and minor elements and nutrients, calcite $\delta^{18}\text{O}$, and fire-sensitive biomarkers. Trace and minor elements and biomarkers are thought to reach stalagmites after originating in burned vegetation and soil and being carried by infiltrating waters through the vadose zone before being sequestered in the growing stalagmites.

Ash and soil leachates confirm that the inorganic fire signal is likely to be originating from the ash, as concentrations of many analytes (including Na, K, Rb, Ba, V, Mn, Co, Ni, Cu, Mo, Si, P, As, Sb, Se, Cl, SO₄) are generally higher in ash leachates than in soil leachates, although there is some variability by location. Additionally, many elements vary with ash colour (itself a proxy for burn severity) suggesting that burn severity as well as fire frequency may be recorded by speleothems, as first suggested by McDonough et al. (2022). While some analytes are both higher in ash leachates than in soil leachates and vary with burn severity (e.g. Na, K, Rb, Mn, P, As, and SO₄) not all may be of sufficient concentration to be detectable by LA-ICP-MS or synchrotron X-ray Fluorescence Microscopy, the standard methods to measure stalagmite trace element.

The pyrogenic biomarkers analysed here (six PAHs and levoglucosan) were in low abundance in the majority of ash leachate samples (see Table S7 for abundances). This may have been due to degradation *ex situ* when stored at laboratory temperatures (Douglas et al., 2018; Rost et al., 2002). The samples that had measurable biomarkers were collected and analysed within two months, a long enough delay that some degradation can be expected to have occurred (Douglas et al., 2018), although repeat analyses of samples presented here suggests that degradation may be non-linear or secondary to sample heterogeneity (see Figure S4.2 in Text S4). Douglas et al. (2018) showed that Chrysene and Pyrene were robust to

degradation under ambient temperatures. Concentrations of both Chrysene and Pyrene in samples presented here were low, and there was no clear trend by ash colour for either compound, although in general black and grey ashes had higher concentrations of both compounds. Considering all PAHs presented here, concentrations tended to be higher in the lower molecular weight compounds, and summed concentrations were highest in black and grey ash samples. This is consistent with both laboratory studies and analysis of wildfire ashes, which have demonstrated that highest PAH concentrations from between 400-600 °C (Karp et al., 2020), and which have shown total concentrations are higher in black ashes than in white ashes (Chen et al., 2018).

Anhydrosugars (including levoglucosan) are reactive and soluble. In open fires, they may appear in all phases (as gas, particles, or in charcoal) (Suciu et al., 2019). Anhydrosugars are released in greatest quantities at ~300 °C (Shafizadeh et al., 1979; Suciu et al., 2019), although a second peak may be observed at 600 °C due to the depolymerisation of polymeric products formed from the thermal conversion of water-soluble compounds (Suciu et al., 2019, p. 213). Suciu et al. (2019) suggest that it is the reaction of these high-temperature anhydrosugars, with aromatic substances which may result in anhydrosugars forming in char. While there is no clear trend in levoglucosan concentration by ash colour, in general concentrations are higher in grey and white ash samples than in black ash samples. As the chemical structure of anhydrosugars means they bond well with chelating metals (e.g. Fe and Al; Suciu et al., 2019), we could have expected that the samples with the highest levoglucosan concentrations would also have high concentrations of Fe and Al. Instead, we find that of those seven samples, the highest concentrations of levoglucosan are found in the sample with the third highest Fe concentrations and the lowest Al concentrations (of the seven Golgotha Cave ash samples presented in section 3.1.3). As for the PAHs, a larger sample size with reduced opportunity for sample degradation is needed to be able to draw stronger conclusions about the use of levoglucosan as a speleothem palaeofire proxy.

That biomarker concentrations may degrade in both collected samples (Douglas et al., 2018; Rost et al., 2002), and *in situ* (Kim et al., 2011; Simon et al., 2016; Yang et al., 2010) should be considered when interpreting them as proxies for past fire. For example, in southwest Western Australia, the bushfire season peaks in summer and autumn. Dripwater monitoring at Golgotha Cave has shown that activation of fractures (and so potentially more efficient transport of the surface fire signal) is generally enhanced when soil stores are saturated (Priestley et al., 2023), which may be months after the fire season has finished. This suggests that where biomarkers are incorporated in speleothems, they may have been degraded prior to inclusion. Additionally, that low molecular weight PAHs are generally more abundant than high molecular weight PAHs, and that total PAH concentrations are higher in black and grey ashes than in white ashes both suggest that PAH-derived records of past fires may be biased towards less-severe burns. Homann et al. (2023) found that high molecular weight PAHs were often <LOD in a Mexican speleothem. They attributed this to filtering of high molecular weight PAHs by overlying soils and epikarst, as earlier suggested by Perrette et al. (2013). Our results suggest that, if speleothem PAHs are derived from the leaching of deposited ashes, high molecular weight PAHs and PAHs sourced from more severe fires are unlikely to be incorporated, as initial concentrations of both are low, and karst processes are likely to further dilute them. While results presented here will be useful for the interpretation of pyrogenic biomarkers in speleothems, more research is needed to better understand the transport and deposition of pyrogenic biomarkers in karst systems.

4.3 Implications for surface and groundwaters

The impact of wildfire on surface waters has been well-documented, and elevated concentrations of contaminants are commonly seen (Beyene et al., 2023; Hickenbottom et al.,

2023), along with increased turbidity (Chen and Chang, 2022; Emmerton et al., 2020) and changes in pH (Costa et al., 2014; Granath et al., 2021), all of which pose risk to both natural and human systems. Karst systems make up 7-12% of the terrestrial earth surface, and ~25% of the world's population rely on karst aquifers for their water supply (Ford and Williams, 2007; Hartmann et al., 2014). While groundwaters are generally thought to be less susceptible to contamination than surface waters (Reberski et al., 2022), contamination of karst groundwaters is a known concern (Vilhar et al., 2022). Contaminants may be both autogenic and allogenic, occurring as both point-source and diffuse sources (Ford and Williams, 2007). Karst aquifers are susceptible to pollution because they very efficiently transport contaminants and they have limited capacity to filter them (Ford and Williams, 2007; Sasowsky, 2000). Karst aquifers have been contaminated by a range of pollutants such as fertilisers, pesticides, pharmaceuticals, microplastics, effluent, and urban and agricultural runoff (Jiménez-Sánchez et al., 2008; Reberski et al., 2022; Panno et al., 2019). That karst aquifers may be more susceptible to contamination than non-karst aquifers is demonstrated by Reberski et al. (2022), who in a review of fifty studies of anthropogenic contaminants in karst aquifers showed that while concentrations of anthropogenic contaminants were lower in karst aquifers than in surface waters, karst aquifers had higher concentrations of those contaminants than other aquifers.

There has been limited research on the impact of fire as a contaminant source in karst aquifers, but land clearing and fire are both thought to result in heightened nutrient loading in karst systems (Gillieson and Thurgate, 1999). In the karst vadose zone, the geochemical response to fires in dripwater is variable, and appears to depend on both the burn severity and the cave depth (Coleborn et al., 2019, 2018; Nagra et al., 2016; Treble et al., 2016). Fires have also been implicated in enhanced recharge in the vadose zone, through heat-induced fracturing of the host rock (McDonough et al., 2022; Meng et al., 2020; Wu and Wang, 2012). McDonough et al. (2022) attributed enhanced organic matter in a speleothem to increased fracture flow following a severe bushfire. Fires have also been implicated in reduced infiltration in karst due to sealing of the epikarst (the uppermost layer of the karst; Holland, 1994), although there has been little reporting of this effect. Metals are listed as a key karst contaminant (Vesper et al., 2003), and results presented here show that post-fire ashes may be a point-source of metal contamination, at concentrations higher than normally found in soils. Concentrations of key potential contaminants (As, Ba, Co, Cu, Mn, Mo, Ni, Sn, V, Zn, P, S, SO₄, Phenanthrene, Anthracene, Pyrene, and Benzopyrene) in both ash and soil leachates are generally lower than the Western Australian Ecological Investigation Levels (Department of Environment and Conservation, 2010; see Table S11), with the exception of S and SO₄, which both exceed the ecological investigation levels. While concentrations are generally low, ash leachate concentrations are much higher than soil leachate concentrations (Table S11), and it is unclear how flushes these potential contaminants might impact the karst environment, including both fragile cave ecosystems and water resources. Further investigation is required at scales ranging from the cave to the catchment to determine whether ash inputs are a significant contamination source for karst aquifers. Since climate change is likely to strain global water resources, and since karst aquifers make such a large contribution to global water resources, understanding how best to minimise their contamination needed to ensure future water security.

5 Conclusion

Ashes from both wild and prescribed fires are sources of both contaminants and potential fire proxies for palaeoenvironmental research. In our analyses of ash leachates from ashes collected in both southwest and southeast Australia, we found that ash leachate inorganic chemistry primarily varies with ash colour (which is an indicator of burn severity)

and location. Statistical difference in inorganic analyte concentration by ash colour was mainly found between the ash colour severity ‘end-members’ (i.e. black vs white ashes). This suggests that palaeoenvironmental applications of the relationships between inorganic ash chemistry and burn severity will likely be limited to being able to differentiate between more and less severe burns.

PCA and Shapley value regression demonstrated that location and, to a lesser extent, fire history also influence inorganic ash leachate chemistry. The PCA demonstrated that while the first PC explained ash colour, the second PC explained location, with samples from southeast Australia clustering differently to samples from southwest Australia. Shapley value regression found that location was the dominant predictor of ash inorganic chemistry, although for most elements, although ash colour was generally the second-most important predictor. It should be noted that the collection of samples from southeast Australia was delayed, and so the time the ashes spent degrading and reacting in the environment may be more important than location, as suggested elsewhere (Sánchez-García et al.; 2023). Fire histories, including the number of years since the last fire, and the total number of fires on record for each collection point, had limited influence on ash leachate inorganic chemistry. This is a positive outcome for palaeoenvironmental applications, as we can assume that there is little memory in the system as fire history was generally a poor predictor of ash and soil chemistry, and the chemistry of ash produced by each fire event should largely be independent of past. This means that relative fire severities at a site should be able to be determined after consideration of any vegetation or land use changes.

The relationship between ash leachate inorganic chemistry and elemental volatilisation temperature did not wholly account for the differences in ash leachates by ash colour. Competing factors which may explain why some analytes are higher in less combusted ashes than in more combusted ashes (or vice versa) include that combustion completeness may be independent of burn temperature, that pH affects the solubility of many elements, that some metals will form complexes with organic matter, and that some ashes potentially degraded prior to sampling (i.e. presumably removal of fine grains and dissolved elements).

A comparison of ash leachate results presented here with those published elsewhere showed significant heterogeneity in ash leachate inorganic geochemistry, including in how geochemistry differed between black and white ashes. This suggests some level of site or regional specificity, which is an important consideration for any palaeofire reconstruction. We do note that our results showed good agreement with Miotliński et al. (2023), the only other analysis of ash leachates from southwest Australia. For most elements, concentrations were higher in ash leachates than in soil leachates. This is important for speleothem palaeofire research, as it suggests the signal is sourced from ash, and not from soil, as seen elsewhere (Hartland et al., 2012). Elements which are higher in soil leachates than in ash leachates (e.g., Fe) may be the key to finger-printing soil geochemical inputs. Key elements which should be considered in future speleothem palaeofire include Na, K, Rb, Mn, P, As, Se, V, and Cl, and SO_4 , as these elements all varied significantly in leachates of black and white ashes, and are all readily measured in calcite via LA-ICP-MS or SIMS (with sulphate measured as elemental S), and are all generally of higher concentrations in ash leachates than in soil leachates.

The preliminary biomarker results presented here were inconclusive, although PAH concentrations were generally higher in black ash samples than in white ash samples, and levoglucosan concentrations were generally higher in grey and white samples than in black samples. While degradation *ex situ* may account for some inconsistency, further analyses are

to establish the potential relationships between these biomarkers and burn severity, how these biomarkers degrade in nature, and the implications of for speleothem palaeofire research.

6 Acknowledgements

This research was funded by the Australian Research Council (DP200100203). MC was supported by an Early Career Research Grant from the Australian Institute of Nuclear Science and Engineering. We thank Yanchep National Parks staff, Calgardup Caves staff, the Kempsey Speleological Society, and Lachie MacCaw for assistance with sample collection. Thanks to Brett Rowling and Chris Vardanega at ANSTO ITNS for analyses of ash leachates. Thanks to Eve Slavich from UNSW Stats Central for statistical advice, and to Morgan Williams for productive conversation on the analysis of compositional data. Thanks also to Cameron Ritchie for helpful pointers on the geology of southwest WA, and to Tim Payne for discussion of leachate chemistry. We respectfully acknowledge the Whadjuk Noongar, Wadandi Noongar, and Dunghutti peoples as the traditional and spiritual custodians of the Yanchep (on Whadjuk Noongar boodja), Margaret River (on Wadandi boodja), and Macleay regions (on Dunghutti lands), where samples were collected for this research.

7 Open research

Data and scripts for the statistical analyses and data visualisation are available at <https://doi.org/10.6084/m9.figshare.25001858> (Campbell et al., 2024). These data are published under a CC BY 4.0 License. **Please note that for the original submission the editor has been supplied with a sharelink to the dataset.**

8 References

- Adams, P.W., Boyle, J.R., 1980. Effects of Fire on Soil Nutrients in Clearcut and Whole-tree Harvest Sites in Central Michigan. *Soil Science Society of America Journal* 44, 847–850. <https://doi.org/10.2136/sssaj1980.03615995004400040038x>
- American Public Health Association, American Water Works Association, Water Environment Federation, Baird, R.B., Eaton, A.D., Rice, E.W. (Eds.), 2017. *Standard Methods for the Examination of Water and Wastewater*, 23rd ed. APHA Press, Washington DC.
- Argiriadis, E., Denniston, R.F., Barbante, C., 2019. Improved Polycyclic Aromatic Hydrocarbon and n-Alkane Determination in Speleothems through Cleanroom Sample Processing. *Anal. Chem.* 91, 7007–7011. <https://doi.org/10.1021/acs.analchem.9b00767>
- Argiriadis, E., Denniston, R.F., Ondeï, S., Bowman, D.M.J.S., Genuzio, G., Nguyen, H.Q.A., Thompson, J., Baltieri, M., Azenon, J., Cugley, J., Woods, D., Humphreys, W.F., Barbante, C., 2023. Polycyclic aromatic hydrocarbons in tropical Australian stalagmites: a framework for reconstructing paleofire activity. *Geochimica et Cosmochimica Acta*. <https://doi.org/10.1016/j.gca.2023.11.033>
- Bai, J., Sun, X., Zhang, C., Xu, Y., Qi, C., 2013. The OH-initiated atmospheric reaction mechanism and kinetics for levoglucosan emitted in biomass burning. *Chemosphere* 93, 2004–2010. <https://doi.org/10.1016/j.chemosphere.2013.07.021>
- Baker, A., Berthelin, R., Cuthbert, M.O., Treble, P.C., Hartmann, A., KSS Cave Studies Team, 2020. Rainfall recharge thresholds in a subtropical climate determined using a regional cave drip water monitoring network. *Journal of Hydrology* 587, 125001. <https://doi.org/10.1016/j.jhydrol.2020.125001>

1045 Balfour, V.N., Woods, S.W., 2013. The hydrological properties and the effects of
 1046 hydration on vegetative ash from the Northern Rockies, USA. *CATENA* 111, 9–24.
 1047 <https://doi.org/10.1016/j.catena.2013.06.014>

1048 Bento-Gonçalves, A., Vieira, A., Úbeda, X., Martin, D., 2012. Fire and soils: Key
 1049 concepts and recent advances. *Geoderma*, Fire effects on soil properties 191, 3–13.
 1050 <https://doi.org/10.1016/j.geoderma.2012.01.004>

1051 Beyene, M.T., Leibowitz, S.G., Dunn, C.J., Bladon, K.D., 2023. To burn or not to
 1052 burn: An empirical assessment of the impacts of wildfires and prescribed fires on trace
 1053 element concentrations in Western US streams. *Science of The Total Environment* 863,
 1054 160731. <https://doi.org/10.1016/j.scitotenv.2022.160731>

1055 Bhattarai, H., Saikawa, E., Wan, X., Zhu, H., Ram, K., Gao, S., Kang, S., Zhang, Q.,
 1056 Zhang, Y., Wu, G., Wang, X., Kawamura, K., Fu, P., Cong, Z., 2019. Levoglucosan as a tracer
 1057 of biomass burning: Recent progress and perspectives. *Atmospheric Research* 220, 20–33.
 1058 <https://doi.org/10.1016/j.atmosres.2019.01.004>

1059 Bivand, R., Keitt, T., Rowlingson, B., 2021. rgdal: Bindings for the “Geospatial” Data
 1060 Abstraction Library.

1061 Blumenstock, M., Zimmermann, R., Schramm, K.-W., Kettrup, A., 2000. Influence of
 1062 combustion conditions on the PCDD/F-, PCB-, PCBz- and PAH-concentrations in the post-
 1063 combustion chamber of a waste incineration pilot plant. *Chemosphere* 40, 987–993.
 1064 [https://doi.org/10.1016/S0045-6535\(99\)00343-4](https://doi.org/10.1016/S0045-6535(99)00343-4)

1065 Bodí, M.B., Martin, D.A., Balfour, V.N., Santín, C., Doerr, S.H., Pereira, P., Cerdà, A.,
 1066 Mataix-Solera, J., 2014. Wildland fire ash: Production, composition and eco-hydro-
 1067 geomorphic effects. *Earth-Science Reviews* 130, 103–127.
 1068 <https://doi.org/10.1016/j.earscirev.2013.12.007>

1069 Bradstock, R.A., Auld, T.D., 1995. Soil Temperatures During Experimental Bushfires
 1070 in Relation to Fire Intensity: Consequences for Legume Germination and Fire Management in
 1071 South-Eastern Australia. *Journal of Applied Ecology* 32, 76–84.
 1072 <https://doi.org/10.2307/2404417>

1073 Broadley, M., Brown, P., Cakmak, I., Rengel, Z., Zhao, F., 2012b. Function of
 1074 Nutrients: Micronutrients, in: Marschner’s Mineral Nutrition of Higher Plants. Elsevier.

1075 Budescu, D.V., 1993. Dominance analysis: A new approach to the problem of relative
 1076 importance of predictors in multiple regression. *Psychological Bulletin* 114, 542–551.
 1077 <https://doi.org/10.1037/0033-2909.114.3.542>

1078 Burton, C.A., Hoefen, T.M., Plumlee, G.S., Baumberger, K.L., Backlin, A.R.,
 1079 Gallegos, E., Fisher, R.N., 2016. Trace Elements in Stormflow, Ash, and Burned Soil
 1080 following the 2009 Station Fire in Southern California. *PLOS ONE* 11, e0153372.
 1081 <https://doi.org/10.1371/journal.pone.0153372>

1082 Campbell, G.S., Jungbauer, J.D.J., Bidlake, W.R., Hungerford, R.D., 1994. Predicting
 1083 the effect of temperature on soil thermal conductivity. *Soil Science* 158, 307.

1084 Campbell, J.B., 1979. Spatial Variability of Soils. *Annals of the Association of*
 1085 *American Geographers* 69, 544–556.

1086 Campbell, M., McDonough, L., Treble, P.C., Baker, A., Kosarac, N., Coleborn, K.,
 1087 Wynn, P.M., Schmitt, A.K., 2023. A Review of Speleothems as Archives for Paleofire

1088 Proxies, With Australian Case Studies. *Reviews of Geophysics* 61, e2022RG000790.
 1089 <https://doi.org/10.1029/2022RG000790>

1090 Campbell, M., Treble, P.C., McDonough, L.K., Naeher, S., Baker, A., Grierson, P.F.,
 1091 Wong, H., Andersen, M.S., 2024. Australian Ash and Soil Leachate data and scripts.
 1092 <https://doi.org/10.6084/m9.figshare.25001858>

1093 Campos, I., Vale, C., Abrantes, N., Keizer, J.J., Pereira, P., 2015. Effects of wildfire on
 1094 mercury mobilisation in eucalypt and pine forests. *CATENA* 131, 149–159.
 1095 <https://doi.org/10.1016/j.catena.2015.02.024>

1096 Canty, A., Ripley, B.D., 2022. boot: Bootstrap R (S-Plus) Functions.

1097 Carpenter, J., Bithell, J., 2000. Bootstrap confidence intervals: when, which, what? A
 1098 practical guide for medical statisticians. *Statistics in Medicine* 19, 1141–1164.
 1099 [https://doi.org/10.1002/\(SICI\)1097-0258\(20000515\)19:9<1141::AID-SIM479>3.0.CO;2-F](https://doi.org/10.1002/(SICI)1097-0258(20000515)19:9<1141::AID-SIM479>3.0.CO;2-F)

1100 Certini, G., 2005. Effects of fire on properties of forest soils: a review. *Oecologia* 143,
 1101 1–10. <https://doi.org/10.1007/s00442-004-1788-8>

1102 Chapin, F.S., Matson, P.A., Vitousek, P.M., 2011. *Principles of Terrestrial Ecosystem*
 1103 *Ecology*. Springer New York, New York, NY. <https://doi.org/10.1007/978-1-4419-9504-9>

1104 Chen, H., Chow, A.T., Li, X.-W., Ni, H.-G., Dahlgren, R.A., Zeng, H., Wang, J.-J.,
 1105 2018. Wildfire Burn Intensity Affects the Quantity and Speciation of Polycyclic Aromatic
 1106 Hydrocarbons in Soils. *ACS Earth Space Chem.* 2, 1262–1270.
 1107 <https://doi.org/10.1021/acsearthspacechem.8b00101>

1108 Coleborn, K., Baker, Andy, Treble, P.C., Andersen, M.S., Baker, Andrew, Tadros,
 1109 C.V., Tozer, M., Fairchild, I.J., Spate, A., Meehan, S., 2019. Corrigendum to “The impact of
 1110 fire on the geochemistry of speleothem-forming drip water in a sub-alpine cave” [*Sci. Total*
 1111 *Environ.* (2018) 408–420]. *Science of The Total Environment* 668, 1339–1340.
 1112 <https://doi.org/10.1016/j.scitotenv.2019.02.350>

1113 Coleborn, K., Baker, Andy, Treble, P.C., Andersen, M.S., Baker, Andrew, Tadros,
 1114 C.V., Tozer, M., Fairchild, I.J., Spate, A., Meehan, S., 2018. The impact of fire on the
 1115 geochemistry of speleothem-forming drip water in a sub-alpine cave. *Science of The Total*
 1116 *Environment* 642, 408–420. <https://doi.org/10.1016/j.scitotenv.2018.05.310>

1117 Croke, J., Vítkovský, J., Hughes, K., Campbell, M., Amirnezhad-Mozhdehi, S.,
 1118 Parnell, A., Cahill, N., Dalla Pozza, R., 2021. A palaeoclimate proxy database for water
 1119 security planning in Queensland Australia. *Sci Data* 8, 292. <https://doi.org/10.1038/s41597-021-01074-8>

1120

1121 Costa, M.R., Calvão, A.R. and Aranha, J., 2014. Linking wildfire effects on soil and
 1122 water chemistry of the Marão River watershed, Portugal, and biomass changes detected from
 1123 Landsat imagery. *Applied Geochemistry* 44, 93–102.
 1124 <https://doi.org/10.1016/j.apgeochem.2013.09.009>

1125 Dasgupta, S., Siegel, D.I., Zhu, C., Chanton, J.P., Glaser, P.H., 2015. Geochemical
 1126 Mixing in Peatland Waters: The Role of Organic Acids. *Wetlands* 35, 567–575.
 1127 <https://doi.org/10.1007/s13157-015-0646-2>

1128 Davison, A.C., Hinkley, D.V., 1997. *Bootstrap Methods and Their Applications*.
 1129 Cambridge University Press, Cambridge.

1130 DeBano, L.F., 2000. The role of fire and soil heating on water repellency in wildland
 1131 environments: a review. *Journal of Hydrology* 231–232, 195–206.
 1132 [https://doi.org/10.1016/S0022-1694\(00\)00194-3](https://doi.org/10.1016/S0022-1694(00)00194-3)

1133 Denis, E.H., Toney, J.L., Taroza, R., Scott Anderson, R., Roach, L.D., Huang, Y.,
 1134 2012. Polycyclic aromatic hydrocarbons (PAHs) in lake sediments record historic fire events:
 1135 Validation using HPLC-fluorescence detection. *Organic Geochemistry* 45, 7–17.
 1136 <https://doi.org/10.1016/j.orggeochem.2012.01.005>

1137 Department of Environment and Conservation, 2010. Assessment levels for Soil,
 1138 Sediment and Water, Contaminated Sites Management Series. Government of Western
 1139 Australia.

1140 Dixon, D.J., Callow, J.N., Duncan, J.M.A., Setterfield, S.A., Pauli, N., 2022.
 1141 Regional-scale fire severity mapping of Eucalyptus forests with the Landsat archive. *Remote*
 1142 *Sensing of Environment* 270, 112863. <https://doi.org/10.1016/j.rse.2021.112863>

1143 Douglas, G., Hardenstine, J., Rouhani, S., Kong, D., Arnold, R., Gala, W., 2018.
 1144 Chemical Preservation of Semi-volatile Polycyclic Aromatic Hydrocarbon Compounds at
 1145 Ambient Temperature: A Sediment Sample Holding Time Study. *Arch Environ Contam*
 1146 *Toxicol* 75, 486–494. <https://doi.org/10.1007/s00244-018-0517-y>

1147 Dunn, O.J., 1964. Multiple Comparisons Using Rank Sums. *Technometrics* 6, 241–
 1148 252. <https://doi.org/10.2307/1266041>

1149 Elias, V.O., Simoneit, B.R.T., Cordeiro, R.C., Turcq, B., 2001. Evaluating
 1150 levoglucosan as an indicator of biomass burning in Carajás, amazônia: a comparison to the
 1151 charcoal record22Associate editor: R. Summons. *Geochimica et Cosmochimica Acta* 65,
 1152 267–272. [https://doi.org/10.1016/S0016-7037\(00\)00522-6](https://doi.org/10.1016/S0016-7037(00)00522-6)

1153 Emmerton, C.A., Cooke, C.A., Hustins, S., Silins, U., Emelko, M.B., Lewis, T., Kruk,
 1154 M.K., Taube, N., Zhu, D., Jackson, B., Stone, M., Kerr, J.G., Orwin, J.F., 2020. Severe
 1155 western Canadian wildfire affects water quality even at large basin scales. *Water Research*
 1156 183, 116071. <https://doi.org/10.1016/j.watres.2020.116071>

1157 Fontaine, J., 2022. Yanchep bushfire analysis – Black Summer final report. Nushfire
 1158 and Natural Hazards CRC, Melbourne.

1159 Ford, D., Williams, P., 2007. *Karst Hydrogeology and Geomorphology*, 1st ed. Wiley.
 1160 <https://doi.org/10.1002/9781118684986>

1161 Gabet, E.J., Bookter, A., 2011. Physical, chemical and hydrological properties of
 1162 Ponderosa pine ash. *International Journal of Wildland Fire* 20, 443–452.
 1163 <https://doi.org/10.1071/WF09105>

1164 Geoscience Australia. (2006). GEODATA TOPO 250K Series 3—(Personal
 1165 Geodatabase format), Geoscience Australia, Canberra, dataset, viewed 18/01/2023. Retrieved
 1166 from <http://pid.geoscience.gov.au/dataset/ga/63999>

1167 Giglio, L., van der Werf, G.R., Randerson, J.T., Collatz, G.J., Kasibhatla, P., 2006.
 1168 Global estimation of burned area using MODIS active fire observations. *Atmospheric*
 1169 *Chemistry and Physics* 6, 957–974. <https://doi.org/10.5194/acp-6-957-2006>

1170 Gillieson, D., Thurgate, M., 1999. Karst and agriculture in Australia. *International*
 1171 *Journal of Speleology* 28. <https://dx.doi.org/10.5038/1827-806X.28.1.11>

- Granath, G., Evans, C.D., Strengbom, J., Fölster, J., Grelle, A., Strömqvist, J., Köhler, S.J., 2021. The impact of wildfire on biogeochemical fluxes and water quality in boreal catchments. *Biogeosciences* 18, 3243–3261. <https://doi.org/10.5194/bg-18-3243-2021>
- Granged, A.J.P., Zavala, L.M., Jordán, A., Bárcenas-Moreno, G., 2011. Post-fire evolution of soil properties and vegetation cover in a Mediterranean heathland after experimental burning: A 3-year study. *Geoderma* 164, 85–94. <https://doi.org/10.1016/j.geoderma.2011.05.017>
- Hageman, P.L., 2007. U.S. Geological Survey Field Leach Test for Assessing Water Reactivity and Leaching Potential of Mine Wastes, Soils, and Other Geologic and Environmental Materials (USGS Numbered Series No. 5-D3), U.S. Geological Survey Field Leach Test for Assessing Water Reactivity and Leaching Potential of Mine Wastes, Soils, and Other Geologic and Environmental Materials, Techniques and Methods. <https://doi.org/10.3133/tm5D3>
- Harris, J.A., 1915. On a Criterion of Substratum Homogeneity (Or Heterogeneity) in Field Experiments. *The American Naturalist* 49, 430–454. <https://doi.org/10.1086/279492>
- Hartland, A., Fairchild, I.J., Lead, J.R., Borsato, A., Baker, A., Frisia, S., Baalousha, M., 2012. From soil to cave: Transport of trace metals by natural organic matter in karst dripwaters. *Chemical Geology* 304–305, 68–82. <https://doi.org/10.1016/j.chemgeo.2012.01.032>
- Hartmann, A., Goldscheider, N., Wagener, T., Lange, J., Weiler, M., 2014. Karst water resources in a changing world: Review of hydrological modeling approaches. *Reviews of Geophysics* 52, 218–242. <https://doi.org/10.1002/2013RG000443>
- Hickenbottom, K., Pagilla, K., Hanigan, D., 2023. Wildfire impact on disinfection byproduct precursor loading in mountain streams and rivers. *Water Research* 244, 120474. <https://doi.org/10.1016/j.watres.2023.120474>
- Hogue, B.A., Inglett, P.W., 2012. Nutrient release from combustion residues of two contrasting herbaceous vegetation types. *Science of The Total Environment* 431, 9–19. <https://doi.org/10.1016/j.scitotenv.2012.04.074>
- Holland, E., 1994. The effects of fire on soluble rock landscapes. *Helictite* 32, 3–10.
- Hollander, M., Wolfe, D.A., 1973. *Nonparametric Statistical Methods*. John Wiley & Sons, New York.
- Homann, J., Karbach, N., Carolin, S.A., James, D.H., Hodell, D., Breitenbach, S.F.M., Kwiecien, O., Brenner, M., Peraza Lope, C., Hoffmann, T., 2023. Past fire dynamics inferred from polycyclic aromatic hydrocarbons and monosaccharide anhydrides in a stalagmite from the archaeological site of Mayapan, Mexico. *Biogeosciences* 20, 3249–3260. <https://doi.org/10.5194/bg-20-3249-2023>
- Homann, J., Oster, J.L., de Wet, C.B., Breitenbach, S.F.M., Hoffmann, T., 2022. Linked fire activity and climate whiplash in California during the early Holocene. *Nat Commun* 13, 1–9. <https://doi.org/10.1038/s41467-022-34950-x>
- Humphreys, F.R., Lambert, M.J., 1965. An examination of a forest site which has exhibited the ash-bed effect. *Soil Res.* 3, 81–94. <https://doi.org/10.1071/sr9650081>
- Jiménez-Sánchez, M., Stoll, H., Vadillo, I., López-Chicano, M., Domínguez-Cuesta, M., Martín-Rosales, W., Meléndez-Asensio, M., 2008. Groundwater contamination in caves:

1215 four case studies in Spain. *International Journal of Speleology* 37.
 1216 <http://dx.doi.org/10.5038/1827-806X.37.1.5>

1217 Johansson, I., van Bavel, B., 2003. Levels and patterns of polycyclic aromatic
 1218 hydrocarbons in incineration ashes. *Science of The Total Environment* 311, 221–231.
 1219 [https://doi.org/10.1016/S0048-9697\(03\)00168-2](https://doi.org/10.1016/S0048-9697(03)00168-2)

1220 Jones, M.W., Abatzoglou, J.T., Veraverbeke, S., Andela, N., Lasslop, G., Forkel, M.,
 1221 Smith, A.J.P., Burton, C., Betts, R.A., van der Werf, G.R., Sitch, S., Canadell, J.G., Santín, C.,
 1222 Kolden, C., Doerr, S.H., Le Quéré, C., 2022. Global and regional trends and drivers of fire
 1223 under climate change. *Reviews of Geophysics* n/a, e2020RG000726.
 1224 <https://doi.org/10.1029/2020RG000726>

1225 Karp, A.T., Holman, A.I., Hopper, P., Grice, K., Freeman, K.H., 2020. Fire
 1226 distinguishers: Refined interpretations of polycyclic aromatic hydrocarbons for paleo-
 1227 applications. *Geochimica et Cosmochimica Acta* 289, 93–113.
 1228 <https://doi.org/10.1016/j.gca.2020.08.024>

1229 Key, C.H., Benson, N.C., 2006. Landscape Assessment (LA) (No. 164), IREMON:
 1230 Fire effects monitoring and inventory system.

1231 Khanna, P.K., Raison, R.J., Falkiner, R.A., 1994. Chemical properties of ash derived
 1232 from Eucalyptus litter and its effects on forest soils. *Forest Ecology and Management*,
 1233 Ameliorative practices for restoring and maintaining 66, 107–125.
 1234 [https://doi.org/10.1016/0378-1127\(94\)90151-1](https://doi.org/10.1016/0378-1127(94)90151-1)

1235 Kim, E.J., Choi, S.-D., Chang, Y.-S., 2011. Levels and patterns of polycyclic aromatic
 1236 hydrocarbons (PAHs) in soils after forest fires in South Korea. *Environ Sci Pollut Res* 18,
 1237 1508–1517. <https://doi.org/10.1007/s11356-011-0515-3>

1238 Kirkby, E., 2012. Introduction, Definition and Classification of Nutrients, in:
 1239 Marschner's Mineral Nutrition of Higher Plants. Elsevier.

1240 Kuo, L.-J., Herbert, B.E., Louchouart, P., 2008. Can levoglucosan be used to
 1241 characterize and quantify char/charcoal black carbon in environmental media? *Organic*
 1242 *Geochemistry* 39, 1466–1478. <https://doi.org/10.1016/j.orggeochem.2008.04.026>

1243 Li, Y., Fu, T.-M., Yu, J.Z., Feng, X., Zhang, L., Chen, J., Boreddy, S.K.R., Kawamura,
 1244 K., Fu, P., Yang, X., Zhu, L., Zeng, Z., 2021. Impacts of Chemical Degradation on the Global
 1245 Budget of Atmospheric Levoglucosan and Its Use As a Biomass Burning Tracer. *Environ.*
 1246 *Sci. Technol.* 55, 5525–5536. <https://doi.org/10.1021/acs.est.0c07313>

1247 Liang, J., 2021. ShapleyValue: Shapley Value Regression for Relative Importance of
 1248 Attributes.

1249 Lipovetsky, S., Conklin, M., 2001. Analysis of regression in game theory approach.
 1250 *Applied Stochastic Models in Business and Industry* 17, 319–330.
 1251 <https://doi.org/10.1002/asmb.446>

1252 Lizundia-Loiola, J., Otón, G., Ramo, R., Chuvieco, E., 2020. A spatio-temporal
 1253 active-fire clustering approach for global burned area mapping at 250 m from MODIS data.
 1254 *Remote Sensing of Environment* 236, 111493. <https://doi.org/10.1016/j.rse.2019.111493>

1255 Marion, G.M., Moreno, J.M., Oechel, W.C., 1991. Fire Severity, Ash Deposition, and
 1256 Clipping Effects on Soil Nutrients in Chaparral. *Soil Science Society of America Journal* 55,
 1257 235–240. <https://doi.org/10.2136/sssaj1991.03615995005500010040x>

1258 Marlon, J.R., Bartlein, P.J., Carcaillet, C., Gavin, D.G., Harrison, S.P., Higuera, P.E.,
 1259 Joos, F., Power, M.J., Prentice, I.C., 2008. Climate and human influences on global biomass
 1260 burning over the past two millennia. *Nature Geosci* 1, 697–702.
 1261 <https://doi.org/10.1038/ngeo313>

1262 McDonough, L.K., Treble, P.C., Baker, A., Borsato, A., Frisia, S., Nagra, G.,
 1263 Coleborn, K., Gagan, M.K., Zhao, J., Paterson, D., 2022. Past fires and post-fire impacts
 1264 reconstructed from a southwest Australian stalagmite. *Geochimica et Cosmochimica Acta*.
 1265 <https://doi.org/10.1016/j.gca.2022.03.020>

1266 Meng, Q.-B., Wang, C.-K., Liu, J.-F., Zhang, M.-W., Lu, M.-M., Wu, Y., 2020.
 1267 Physical and micro-structural characteristics of limestone after high temperature exposure.
 1268 *Bull Eng Geol Environ* 79, 1259–1274. <https://doi.org/10.1007/s10064-019-01620-0>

1269 Millard, S.P., 2013. *EnvStats: An R Package for Environmental Statistics*. Springer,
 1270 New York.

1271 Miotliński, K., Tshering, K., Boyce, M.C., Blake, D., Horwitz, P., 2023. Simulated
 1272 temperatures of forest fires affect water solubility in soil and litter. *Ecological Indicators* 150,
 1273 110236. <https://doi.org/10.1016/j.ecolind.2023.110236>

1274 Misra, M.K., Ragland, K.W., Baker, A.J., 1993. Wood ash composition as a function
 1275 of furnace temperature. *Biomass and Bioenergy, Biomass in Combustion: The Challenge of*
 1276 *Biomass?* 4, 103–116. [https://doi.org/10.1016/0961-9534\(93\)90032-Y](https://doi.org/10.1016/0961-9534(93)90032-Y)

1277 Muñoz-Rojas, M., Erickson, T.E., Martini, D., Dixon, K.W., Merritt, D.J., 2016. Soil
 1278 physicochemical and microbiological indicators of short, medium and long term post-fire
 1279 recovery in semi-arid ecosystems. *Ecological Indicators* 63, 14–22.
 1280 <https://doi.org/10.1016/j.ecolind.2015.11.038>

1281 Nagra, G., Treble, P.C., Andersen, M.S., Fairchild, I.J., Coleborn, K., Baker, A., 2016.
 1282 A post-wildfire response in cave dripwater chemistry. *Hydrol. Earth Syst. Sci.* 20, 2745–
 1283 2758. <https://doi.org/10.5194/hess-20-2745-2016>

1284 NSW Department of Environment, Climate Change, and Water, 2011. *Guide to New*
 1285 *South Wales Karst and Caves*.

1286 NSW Rural Fire Service, 2020. Spring fires torment northern NSW. *Bush Fire bulletin*
 1287 42, 8–9.

1288 Otto, A., Gondokusumo, R., Simpson, M.J., 2006. Characterization and quantification
 1289 of biomarkers from biomass burning at a recent wildfire site in Northern Alberta, Canada.
 1290 *Applied Geochemistry* 21, 166–183. <https://doi.org/10.1016/j.apgeochem.2005.09.007>

1291 Panno, S.V., Kelly, W.R., Scott, J., Zheng, W., McNeish, R.E., Holm, N., Hoellein,
 1292 T.J., Baranski, E.L., 2019. Microplastic Contamination in Karst Groundwater Systems.
 1293 *Groundwater* 57, 189–196. <https://doi.org/10.1111/gwat.12862>

1294 Pebesma, E., 2018. Simple Features for R: Standardized Support for Spatial Vector
 1295 Data. *The R Journal* 10, 439–446. <https://doi.org/10.32614/RJ-2018-009>

1296 Pebesma, E., Bivand, R., 2023. *Spatial Data Science: With Applications in R*, 1st ed.
 1297 Chapman and Hall/CRC, Boca Raton. <https://doi.org/10.1201/9780429459016>

1298 Pellegrini, A.F.A., Harden, J., Georgiou, K., Hemes, K.S., Malhotra, A., Nolan, C.J.,
 1299 Jackson, R.B., 2022. Fire effects on the persistence of soil organic matter and long-term
 1300 carbon storage. *Nat. Geosci.* 15, 5–13. <https://doi.org/10.1038/s41561-021-00867-1>

1301 Pereira, P., Úbeda, X., 2010. Spatial distribution of heavy metals released from ashes
 1302 after a wildfire. *Journal of Environmental Engineering and Landscape Management* 18, 13–
 1303 22. <https://doi.org/10.3846/jeelm.2010.02>
 1304 Pereira, P., Úbeda, X., Martin, D.A., 2012. Fire severity effects on ash chemical
 1305 composition and water-extractable elements. *Geoderma*, Fire effects on soil properties 191,
 1306 105–114. <https://doi.org/10.1016/j.geoderma.2012.02.005>
 1307 Perrette, Y., Poulenard, J., Saber, A.-I., Fanget, B., Guittonneau, S., Ghaleb, B.,
 1308 Garaudee, S., 2008. Polycyclic Aromatic Hydrocarbons in stalagmites: Occurrence and use
 1309 for analyzing past environments. *Chemical Geology* 251, 67–76.
 1310 <https://doi.org/10.1016/j.chemgeo.2008.02.013>
 1311 Perrette, Y., Poulenard, J., Durand, A., Quiers, M., Malet, E., Fanget, B., Naffrechoux,
 1312 E., 2013. Atmospheric sources and soil filtering of PAH content in karst seepage waters.
 1313 *Organic Geochemistry* 65, 37–45. <https://doi.org/10.1016/j.orggeochem.2013.10.005>
 1314 Playford, P.E., Cockbain, A.E., Low, G.H., 1976. Geology of the Perth Basin Western
 1315 Australia (Bulletin No. 124). Geological Survey of Western Australia.
 1316 Priestley, S.C., Treble, P.C., Griffiths, A.D., Baker, A., Abram, N.J., Meredith, K.T.,
 1317 2023. Caves demonstrate decrease in rainfall recharge of southwest Australian groundwater is
 1318 unprecedented for the last 800 years. *Commun Earth Environ* 4, 1–12.
 1319 <https://doi.org/10.1038/s43247-023-00858-7>
 1320 Puth, M.-T., Neuhäuser, M., Ruxton, G.D., 2015. On the variety of methods for
 1321 calculating confidence intervals by bootstrapping. *Journal of Animal Ecology* 84, 892–897.
 1322 <https://doi.org/10.1111/1365-2656.12382>
 1323 QGIS Development Team, 2022. QGIS Geographic Information System, version 3.28.
 1324 QGIS Association.
 1325 Qian, Y., Miao, S.L., Gu, B., Li, Y.C., 2009. Effects of Burn Temperature on Ash
 1326 Nutrient Forms and Availability from Cattail (*Typha domingensis*) and Sawgrass (*Cladium*
 1327 *jamaicense*) in the Florida Everglades. *Journal of Environmental Quality* 38, 451–464.
 1328 <https://doi.org/10.2134/jeq2008.0126>
 1329 Quintana, J.R., Cala, V., Moreno, A.M., Parra, J.G., 2007. Effect of heating on mineral
 1330 components of the soil organic horizon from a Spanish juniper (*Juniperus thurifera* L.)
 1331 woodland. *Journal of Arid Environments* 71, 45–56.
 1332 <https://doi.org/10.1016/j.jaridenv.2007.03.002>
 1333 R Core Team, 2023. R: A Language and Environment for Statistical Computing. R
 1334 Foundation for Statistical Computing, Vienna, Austria.
 1335 Reberski, J., Terzić, J., Maurice, L.D., Lapworth, D.J., 2022. Emerging organic
 1336 contaminants in karst groundwater: A global level assessment. *Journal of Hydrology* 604,
 1337 127242. <https://doi.org/10.1016/j.jhydrol.2021.127242>
 1338 Rehn, E., Rowe, C., Ulm, S., Woodward, C., Bird, M., 2021. A late-Holocene
 1339 multiproxy fire record from a tropical savanna, eastern Arnhem Land, Northern Territory,
 1340 Australia. *The Holocene* 31, 870–883. <https://doi.org/10.1177/0959683620988030>
 1341 Rey-Salgueiro, L., Martínez-Carballo, E., Merino, A., Vega, J.A., Fonturbel, M.T.,
 1342 Simal-Gandara, J., 2018. Polycyclic Aromatic Hydrocarbons in Soil Organic Horizons
 1343 Depending on the Soil Burn Severity and Type of Ecosystem. *Land Degradation &*
 1344 *Development* 29, 2112–2123. <https://doi.org/10.1002/ldr.2806>

1345 Roshan, A., Biswas, A., 2023. Fire-induced geochemical changes in soil: Implication
 1346 for the element cycling. *Science of The Total Environment* 868, 161714.
 1347 <https://doi.org/10.1016/j.scitotenv.2023.161714>

1348 Rosner, B., 1983. Percentage Points for a Generalized ESD Many-Outlier Procedure.
 1349 *Technometrics* 25, 165–172. <https://doi.org/10.1080/00401706.1983.10487848>

1350 Rost, H., Loibner, A.P., Hasinger, M., Braun, R., Szolar, O.H.J., 2002. Behavior of
 1351 PAHs during cold storage of historically contaminated soil samples. *Chemosphere* 49, 1239–
 1352 1246. [https://doi.org/10.1016/S0045-6535\(02\)00497-6](https://doi.org/10.1016/S0045-6535(02)00497-6)

1353 Roy, D.P., Boschetti, L., Maier, S.W., Smith, A.M.S., 2010. Field estimation of ash
 1354 and char colour-lightness using a standard grey scale. *Int. J. Wildland Fire* 19, 698.
 1355 <https://doi.org/10.1071/WF09133>

1356 Rubino, M., D’Onofrio, A., Seki, O., Bendle, J.A., 2016. Ice-core records of biomass
 1357 burning. *The Anthropocene Review* 3, 140–162. <https://doi.org/10.1177/2053019615605117>

1358 Sánchez-García, C., Santín, C., Neris, J., Sigmund, G., Otero, X.L., Manley, J.,
 1359 González-Rodríguez, G., Belcher, C.M., Cerdà, A., Marcotte, A.L., Murphy, S.F., Rhoades,
 1360 C.C., Sheridan, G., Strydom, T., Robichaud, P.R., Doerr, S.H., 2023. Chemical characteristics
 1361 of wildfire ash across the globe and their environmental and socio-economic implications.
 1362 *Environment International* 178, 108065. <https://doi.org/10.1016/j.envint.2023.108065>

1363 Santín, C., Doerr, S.H., Otero, X.L., Chafer, C.J., 2015. Quantity, composition and
 1364 water contamination potential of ash produced under different wildfire severities.
 1365 *Environmental Research* 142, 297–308. <https://doi.org/10.1016/j.envres.2015.06.041>

1366 Santín, C., Doerr, S.H., Shakesby, R.A., Bryant, R., Sheridan, G.J., Lane, P.N.J.,
 1367 Smith, H.G., Bell, T.L., 2012. Carbon loads, forms and sequestration potential within ash
 1368 deposits produced by wildfire: new insights from the 2009 ‘Black Saturday’ fires, Australia.
 1369 *Eur J Forest Res* 131, 1245–1253. <https://doi.org/10.1007/s10342-012-0595-8>

1370 Sasowsky, I.D. (Ed.), 2000. Groundwater flow and contaminant transport in carbonate
 1371 aquifers. Balkema, Rotterdam.

1372 Serrasolsas, I., Khanna, P.K., 1995. Changes in heated and autoclaved forest soils of
 1373 S.E. Australia. II. Phosphorus and phosphatase activity. *Biogeochemistry* 29, 25–41.
 1374 <https://doi.org/10.1007/BF00002592>

1375 Shafizadeh, F., Furneaux, R.H., Cochran, T.G., Scholl, J.P., Sakai, Y., 1979.
 1376 Production of levoglucosan and glucose from pyrolysis of cellulosic materials. *Journal of*
 1377 *Applied Polymer Science* 23, 3525–3539. <https://doi.org/10.1002/app.1979.070231209>

1378 Shakesby, R.A., Doerr, S.H., 2006. Wildfire as a hydrological and geomorphological
 1379 agent. *Earth-Science Reviews* 74, 269–307. <https://doi.org/10.1016/j.earscirev.2005.10.006>

1380 Shi, K., Touge, Y., 2022. Characterization of global wildfire burned area
 1381 spatiotemporal patterns and underlying climatic causes. *Sci Rep* 12, 644.
 1382 <https://doi.org/10.1038/s41598-021-04726-2>

1383 Simon, E., Choi, S.-D., Park, M.-K., 2016. Understanding the fate of polycyclic
 1384 aromatic hydrocarbons at a forest fire site using a conceptual model based on field
 1385 monitoring. *Journal of Hazardous Materials* 317, 632–639.
 1386 <https://doi.org/10.1016/j.jhazmat.2016.06.030>

1387 Simoneit, B.R.T., Schauer, J.J., Nolte, C.G., Oros, D.R., Elias, V.O., Fraser, M.P.,
 1388 Rogge, W.F., Cass, G.R., 1999. Levoglucosan, a tracer for cellulose in biomass burning and

1389 atmospheric particles. *Atmospheric Environment* 33, 173–182.
1390 [https://doi.org/10.1016/S1352-2310\(98\)00145-9](https://doi.org/10.1016/S1352-2310(98)00145-9)

1391 Stronach, N.R.H., McNaughton, S.J., 1989. Grassland Fire Dynamics in the Serengeti
1392 Ecosystem, and a Potential Method of Retrospectively Estimating Fire Energy. *Journal of*
1393 *Applied Ecology* 26, 1025–1033. <https://doi.org/10.2307/2403709>

1394 Suci, L.G., Masiello, C.A., Griffin, R.J., 2019. Anhydrosugars as tracers in the Earth
1395 system. *Biogeochemistry* 146, 209–256. <https://doi.org/10.1007/s10533-019-00622-0>

1396 Treble, P.C., Fairchild, I.J., Baker, A., Meredith, K.T., Andersen, M.S., Salmon, S.U.,
1397 Bradley, C., Wynn, P.M., Hankin, S.I., Wood, A., McGuire, E., 2016. Roles of forest
1398 bioproductivity, transpiration and fire in a nine-year record of cave dripwater chemistry from
1399 southwest Australia. *Geochimica et Cosmochimica Acta* 184, 132–150.
1400 <https://doi.org/10.1016/j.gca.2016.04.017>

1401 Úbeda, X., Pereira, P., Outeiro, L., Martin, D.A., 2009. Effects of fire temperature on
1402 the physical and chemical characteristics of the ash from two plots of cork oak (*Quercus*
1403 *suber*). *Land Degradation & Development* 20, 589–608. <https://doi.org/10.1002/ldr.930>

1404 Ulery, A.L., Graham, R.C., Amrhein, C., 1993. Wood-ash composition and soil pH
1405 following intense burning. *Soil Science* 156, 358–364.

1406 Vachula, R.S., Huang, Y., Longo, W.M., Dee, S.G., Daniels, W.C., Russell, J.M.,
1407 2019. Evidence of Ice Age humans in eastern Beringia suggests early migration to North
1408 America. *Quaternary Science Reviews* 205, 35–44.
1409 <https://doi.org/10.1016/j.quascirev.2018.12.003>

1410 Vesper, D.J., Loop, C.M., White, W.B., 2003. Contaminant transport in karst aquifers.
1411 *Speleogenesis and Evolution of Karst Aquifers* 1, 2–11.

1412 Vilhar, U., Kermavnar, J., Kozamernik, E., Petrič, M., Ravbar, N., 2022. The effects
1413 of large-scale forest disturbances on hydrology – An overview with special emphasis on karst
1414 aquifer systems. *Earth-Science Reviews* 235, 104243.
1415 <https://doi.org/10.1016/j.earscirev.2022.104243>

1416 Vu, V.Q., 2011. ggbiplot: A ggplot2 based biplot.

1417 Wakeham, S.G., Schaffner, C., Giger, W., 1980. Polycyclic aromatic hydrocarbons in
1418 Recent lake sediments—I. Compounds having anthropogenic origins. *Geochimica et*
1419 *Cosmochimica Acta* 44, 403–413. [https://doi.org/10.1016/0016-7037\(80\)90040-X](https://doi.org/10.1016/0016-7037(80)90040-X)

1420 Wei, M., Zhang, Z., Long, T., He, G., Wang, G., 2021. Monitoring Landsat Based
1421 Burned Area as an Indicator of Sustainable Development Goals. *Earth's Future* 9.
1422 <https://doi.org/10.1029/2020EF001960>

1423 Wickham, H., 2022. stringr: Simple, Consistent Wrappers for Common String
1424 Operations.

1425 Wickham, H., 2016. ggplot2: Elegant Graphics for Data Analysis.

1426 Wickham, H., Francois, R., Henry, L., Muller, K., 2020. dplyr: A Grammar of Data
1427 Manipulation.

1428 Wickham, H., Henry, L., 2023. purrr: Functional Programming Tools.

1429 Wickham, H., Hester, J., Bryan, J., 2023. readr: Read Rectangular Text Data.

1430 Williams, P.R., Congdon, R.A., Grice, A.C., Clarke, P.J., 2004. Soil temperature and
1431 depth of legume germination during early and late dry season fires in a tropical eucalypt

1432 savanna of north-eastern Australia. *Austral Ecology* 29, 258–263.
 1433 <https://doi.org/10.1111/j.1442-9993.2004.01343.x>

1434 Wu, G., Wang, D.Y., 2012. Mechanical and Acoustic Emission Characteristics of
 1435 Limestone after High Temperature. *Advanced Materials Research* 446–449, 23–28.
 1436 <https://doi.org/10.4028/www.scientific.net/AMR.446-449.23>

1437 Yang, Y., Zhang, N., Xue, M., Tao, S., 2010. Impact of soil organic matter on the
 1438 distribution of polycyclic aromatic hydrocarbons (PAHs) in soils. *Environmental Pollution*,
 1439 Advances of air pollution science: from forest decline to multiple-stress effects on forest
 1440 ecosystem services 158, 2170–2174. <https://doi.org/10.1016/j.envpol.2010.02.019>

1441 Yusiharni, E., Gilkes, R., 2012. Minerals in the ash of Australian native plants.
 1442 *Geoderma* 189–190, 369–380. <https://doi.org/10.1016/j.geoderma.2012.06.035>

1443 Zennaro, P., Kehrwald, N., Marlon, J., Ruddiman, W.F., Brücher, T., Agostinelli, C.,
 1444 Dahl-Jensen, D., Zangrando, R., Gambaro, A., Barbante, C., 2015. Europe on fire three
 1445 thousand years ago: Arson or climate? *Geophysical Research Letters* 42, 5023–2033.
 1446 <https://doi.org/10.1002/2015GL064259>

1447 Zomer, R.J., Xu, J., Trabucco, A., 2022. Version 3 of the Global Aridity Index and
 1448 Potential Evapotranspiration Database. *Sci Data* 9, 409. [https://doi.org/10.1038/s41597-022-](https://doi.org/10.1038/s41597-022-01493-1)
 1449 [01493-1](https://doi.org/10.1038/s41597-022-01493-1)

1450 **9 References from the Supporting Information**

1451 Alshehri, T., Wang, J., Singerling, S.A., Gigault, J., Webster, J.P., Matiassek, S.J.,
 1452 Alpers, C.N., Baalousha, M., 2023. Wildland-urban interface fire ashes as a major source of
 1453 incidental nanomaterials. *Journal of Hazardous Materials* 443, 130311.
 1454 <https://doi.org/10.1016/j.jhazmat.2022.130311>

1455 Balfour, V.N., Woods, S.W., 2013. The hydrological properties and the effects of
 1456 hydration on vegetative ash from the Northern Rockies, USA. *CATENA* 111, 9–24.
 1457 <https://doi.org/10.1016/j.catena.2013.06.014>

1458 Burton, C.A., Hoefen, T.M., Plumlee, G.S., Baumberger, K.L., Backlin, A.R.,
 1459 Gallegos, E., Fisher, R.N., 2016. Trace Elements in Stormflow, Ash, and Burned Soil
 1460 following the 2009 Station Fire in Southern California. *PLOS ONE* 11, e0153372.
 1461 <https://doi.org/10.1371/journal.pone.0153372>

1462 Douglas, G., Hardenstine, J., Rouhani, S., Kong, D., Arnold, R., Gala, W., 2018.
 1463 Chemical Preservation of Semi-volatile Polycyclic Aromatic Hydrocarbon Compounds at
 1464 Ambient Temperature: A Sediment Sample Holding Time Study. *Arch Environ Contam*
 1465 *Toxicol* 75, 486–494. <https://doi.org/10.1007/s00244-018-0517-y>

1466 Johansen, M.P., Hakonson, T.E., Whicker, F.W., Breshears, D.D., 2003. Pulsed
 1467 Redistribution of a Contaminant Following Forest Fire: Cesium-137 in Runoff. *Journal of*
 1468 *Environmental Quality* 32, 2150–2157.

1469 Ku, P., Tsui, M.T.-K., Nie, X., Chen, H., Hoang, T.C., Blum, J.D., Dahlgren, R.A.,
 1470 Chow, A.T., 2018. Origin, Reactivity, and Bioavailability of Mercury in Wildfire Ash.
 1471 *Environ. Sci. Technol.* 52, 14149–14157. <https://doi.org/10.1021/acs.est.8b03729>

1472 Miotliński, K., Tshering, K., Boyce, M.C., Blake, D., Horwitz, P., 2023. Simulated
 1473 temperatures of forest fires affect water solubility in soil and litter. *Ecological Indicators* 150,
 1474 110236. <https://doi.org/10.1016/j.ecolind.2023.110236>

- Pebesma, E., 2018. Simple Features for R: Standardized Support for Spatial Vector Data. *The R Journal* 10, 439–446. <https://doi.org/10.32614/RJ-2018-009>
- Pebesma, E., Bivand, R., 2023. *Spatial Data Science: With Applications in R*, 1st ed. Chapman and Hall/CRC, Boca Raton. <https://doi.org/10.1201/9780429459016>
- Pereira, P., Úbeda, X., Martín, D.A., 2012. Fire severity effects on ash chemical composition and water-extractable elements. *Geoderma, Fire effects on soil properties* 191, 105–114. <https://doi.org/10.1016/j.geoderma.2012.02.005>
- Quintana, J.R., Cala, V., Moreno, A.M., Parra, J.G., 2007. Effect of heating on mineral components of the soil organic horizon from a Spanish juniper (*Juniperus thurifera* L.) woodland. *Journal of Arid Environments* 71, 45–56. <https://doi.org/10.1016/j.jaridenv.2007.03.002>
- Sánchez-García, C., Santín, C., Neris, J., Sigmund, G., Otero, X.L., Manley, J., González-Rodríguez, G., Belcher, C.M., Cerdà, A., Marcotte, A.L., Murphy, S.F., Rhoades, C.C., Sheridan, G., Strydom, T., Robichaud, P.R., Doerr, S.H., 2023. Chemical characteristics of wildfire ash across the globe and their environmental and socio-economic implications. *Environment International* 178, 108065. <https://doi.org/10.1016/j.envint.2023.108065>
- Úbeda, X., Pereira, P., Outeiro, L., Martín, D.A., 2009. Effects of fire temperature on the physical and chemical characteristics of the ash from two plots of cork oak (*Quercus suber*). *Land Degradation & Development* 20, 589–608. <https://doi.org/10.1002/ldr.930>
- Wickham, H., 2016. *ggplot2: Elegant Graphics for Data Analysis*.
- Wickham, H., Francois, R., Henry, L., Muller, K., 2020. *dplyr: A Grammar of Data Manipulation*.